Sunyaev-Zeldovich Effect Survey Results from Bolocam

Sunil Golwala

KICP Friday Seminar

April 4, 2008

Overview

- Review of the SZ effect
- Applications of the SZ effect
- Bolocam instrument description
- Sky noise removal and analysis techniques
- Constraints on SZ anisotropy
- Upcoming work

The Sunyaev-Zeldovich Effect in Galaxy Clusters

- Thermal SZE is the Compton up-scattering of CMB photons by hot electrons in the intracluster plasma
- $\Delta T_{CMB}/T_{CMB}$ depends only on cluster y (line-of-sight integral of $n_e T_e$). Both ΔT_{CMB} and T_{CMB} are redshifted as photons propagate from clusters, so ratio is independent of distance.
- Thermal SZE causes nonthermal change in spectrum

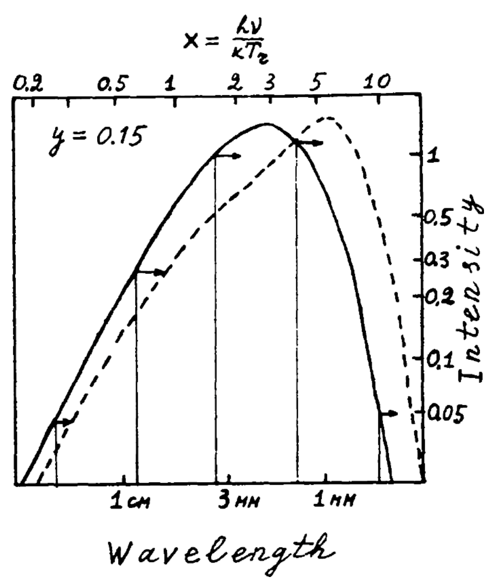

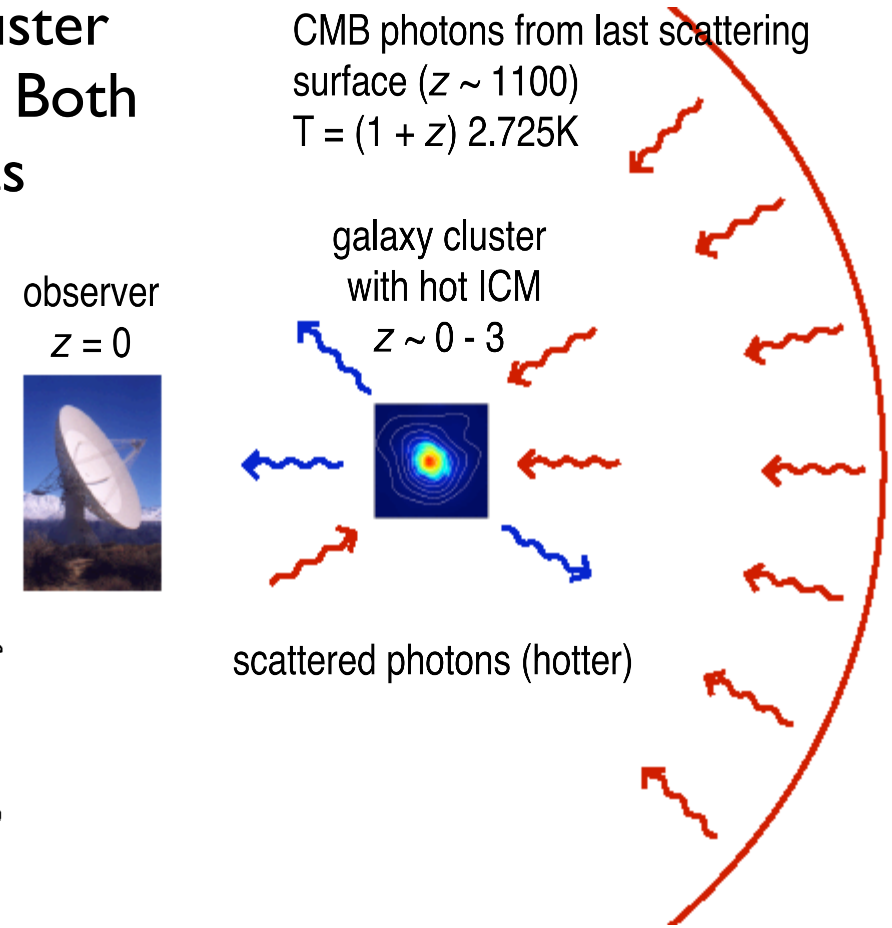

The Sunyaev-Zeldovich Effect in Galaxy Clusters

BIMA SZ + ROSAT X-ray

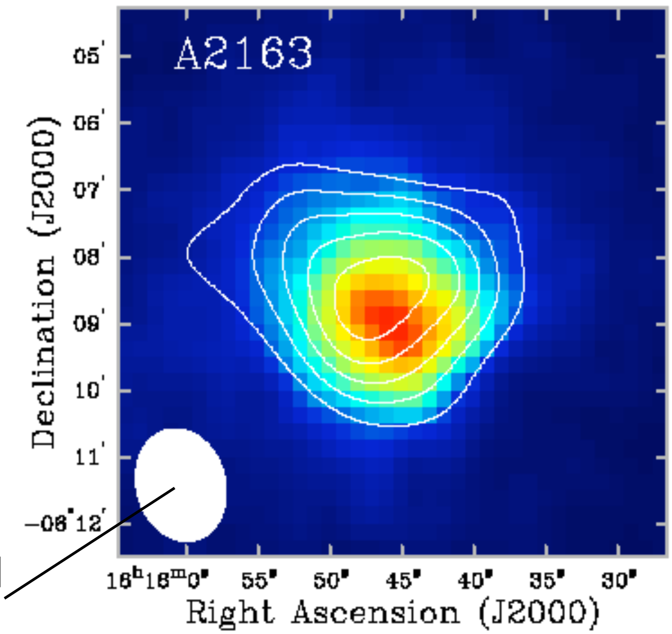

FWHM beam

SuZIE, DIABOLO, and BIMA spectral points

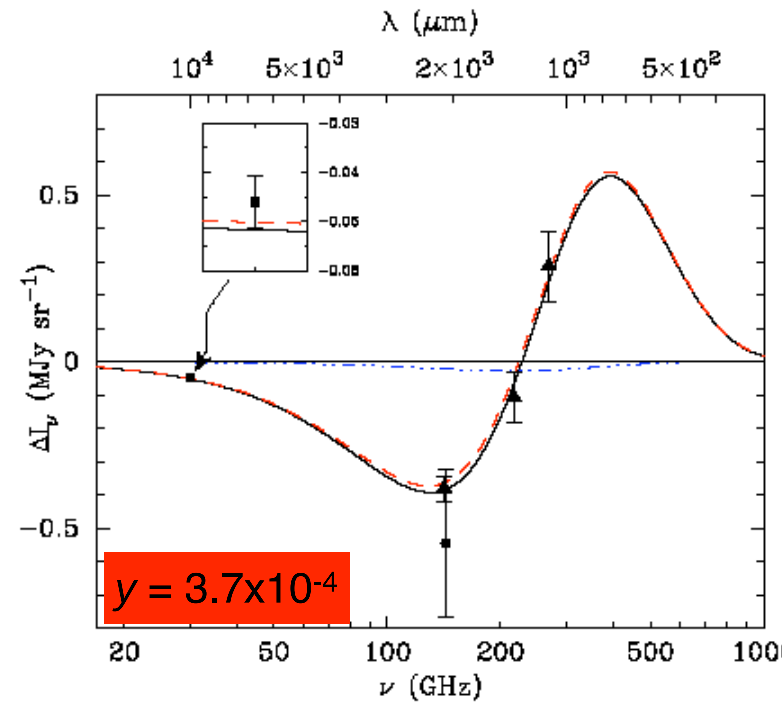

Reese *et al*, LaRoque *et al*

- Beautiful images of SZ from Chicago group using OVRO/BIMA interferometers at 30 GHz
- Spectrum confirmed by measurements from RJ tail through null
- To date, only seen in pointed observations of massive clusters

Applications of the SZ Effect

- Cluster astrophysics
  - measures pressure
  - scaling relations
- Cosmology
  - Hubble constant (geometric effect, with X-ray)
  - Baryon fraction (now measured better by CMB)
  - Evolution of cluster abundance as a probe of dark energy

Studying Clusters with the SZ Effect

Clusters are complicated objects!

SZ measures pressure, in contrast to other observables

gas density

galaxies

SZ ~ n T
(gas pressure)

X-ray
$\sim n^2 \sqrt{T}$

Martin White, Berkeley
http://astron.berkeley.edu/~mwhite/clusterform.html

10 Mpc/h comoving

Studying Clusters with the SZ Effect

Clusters are complicated objects!

SZ measures pressure, in contrast to other observables

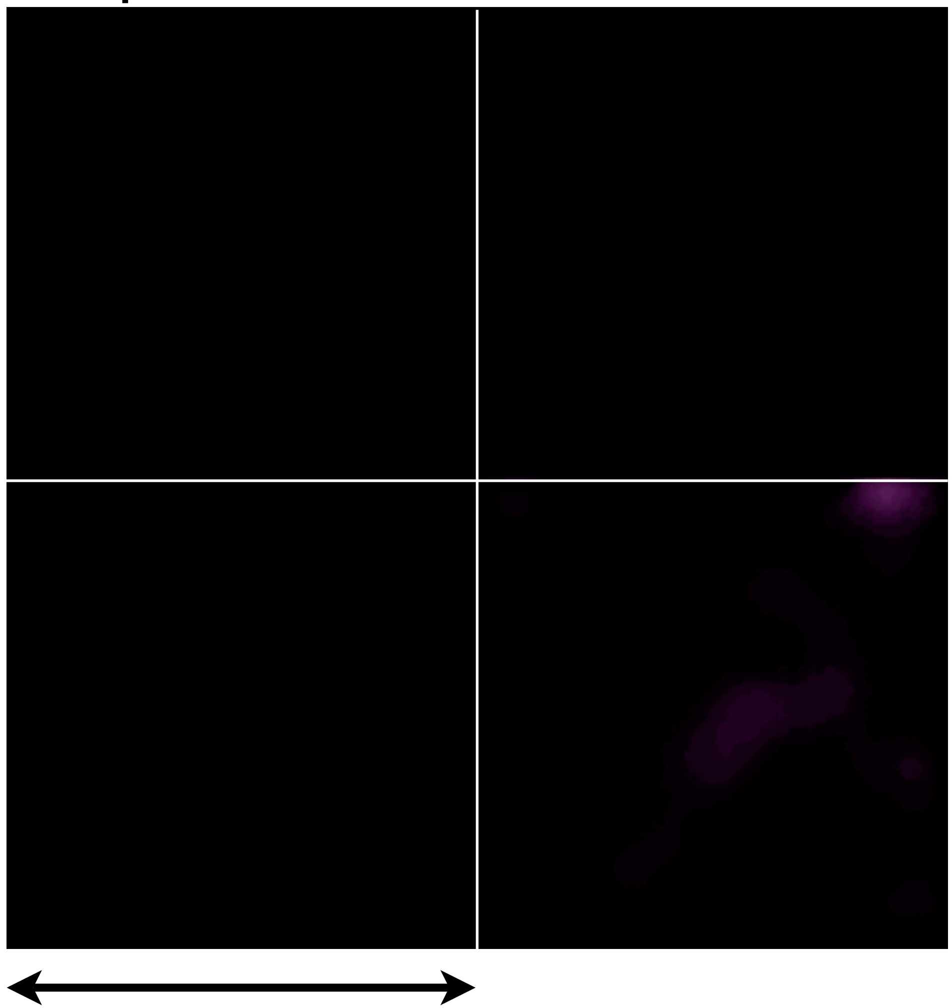

Martin White, Berkeley
http://astron.berkeley.edu/~mwhite/clusterform.html

Studying Clusters with the SZ Effect: Scaling Relations

- SuZIE (S. Church, Stanford)

Benson *et al*, *ApJ* 617:829 (2004)

  - published 11 clusters at 150/220/275(350) GHz, observed SZ flux-T_X scaling relation, but not an imaging experiment

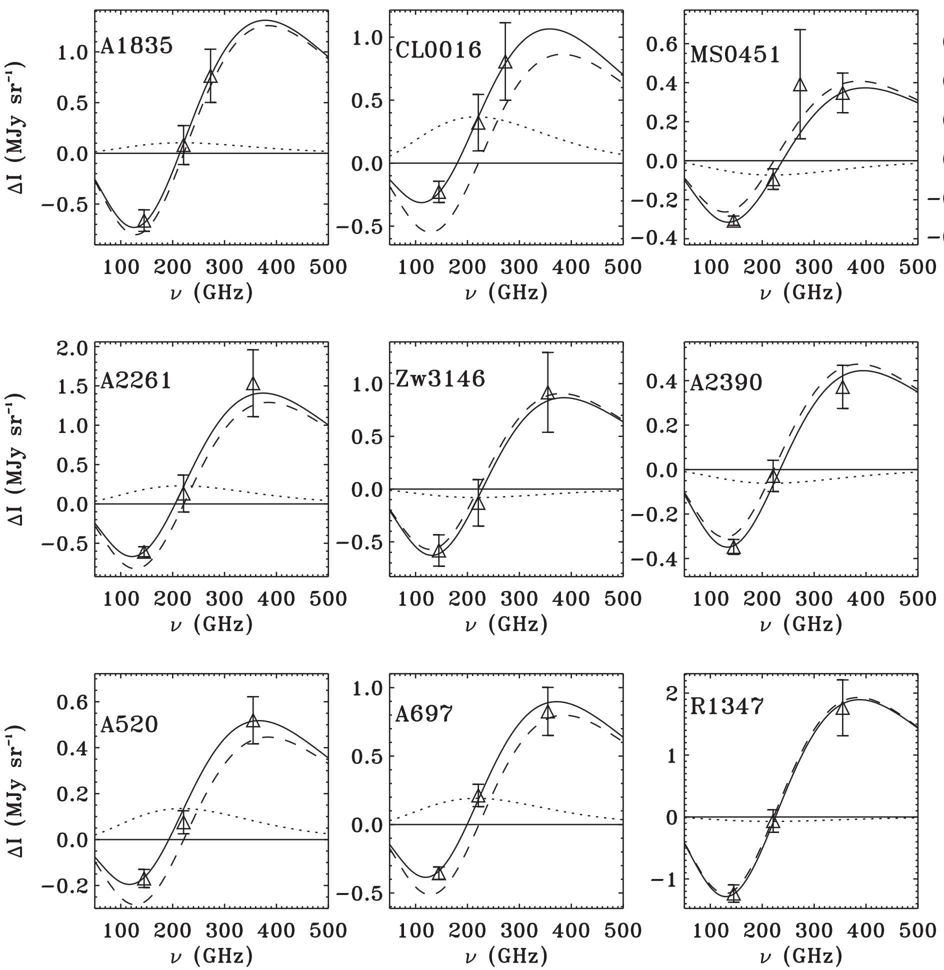

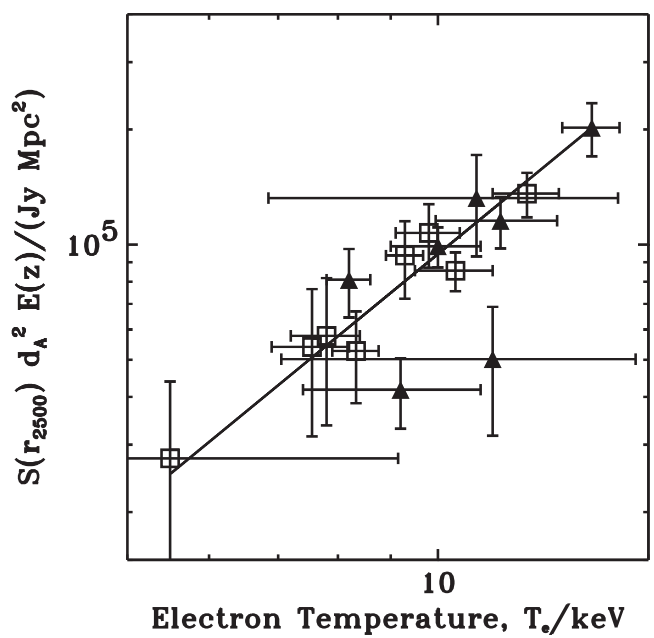

Probing Dark Energy via the Growth of Structure

Virgo Consortium
http://www.icc.dur.ac.uk/Outreach/Movies.html

Probing Dark Energy via the Growth of Structure

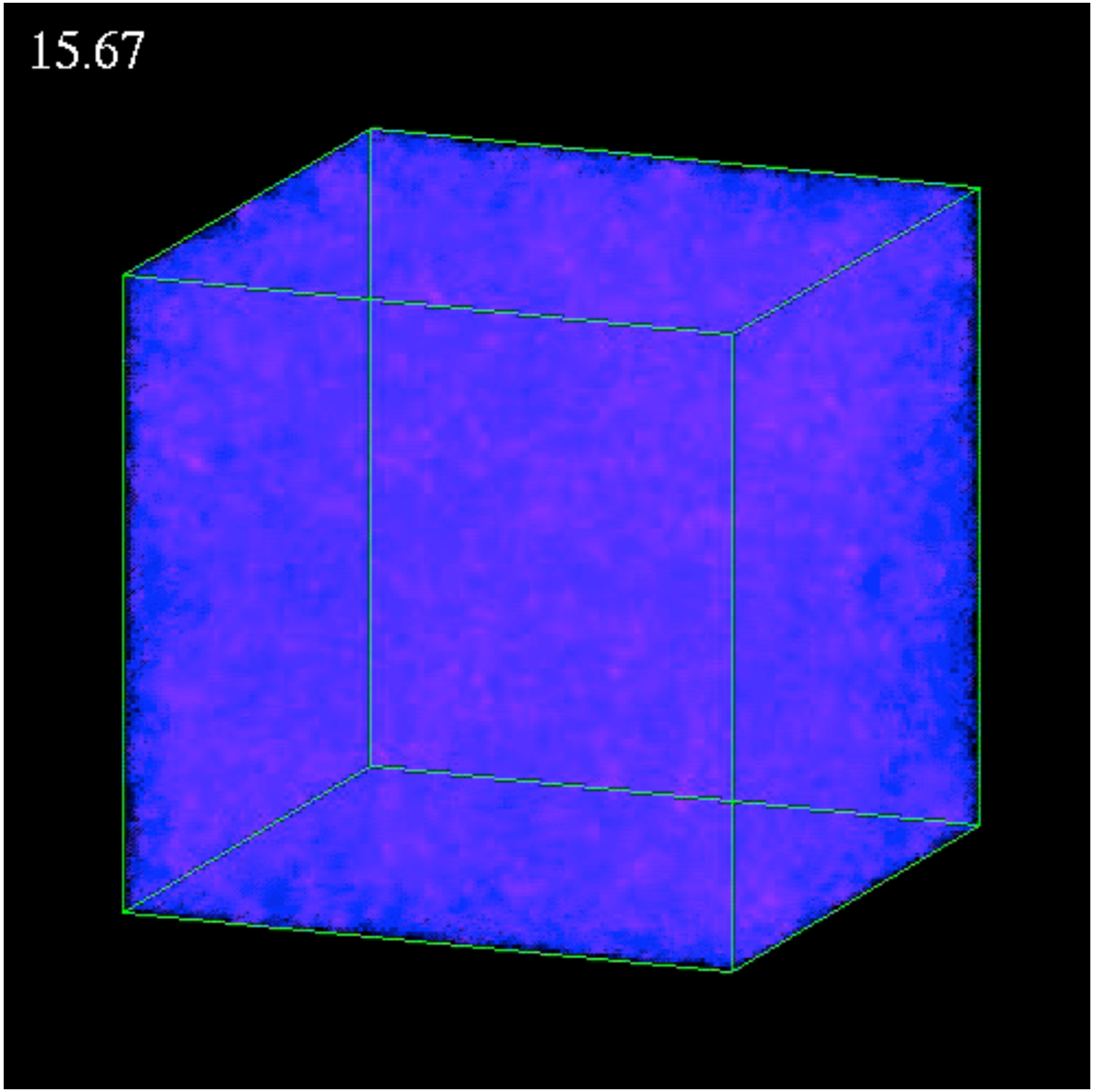

Virgo Consortium
http://www.icc.dur.ac.uk/Outreach/Movies.html

Using Cluster Abundance for Cosmology

- Very sensitive to normalization of power spectrum, and thus to growth function, because clusters are statistically rare excursions
- Clusters form recently ($z < 2$) and so abundance influenced by recent dark-energy domination
- Has historically been a robust predictor of low matter density

Number of clusters per redshift bin above 3.5×10^{14} M_{Sun} in 4000 deg^2

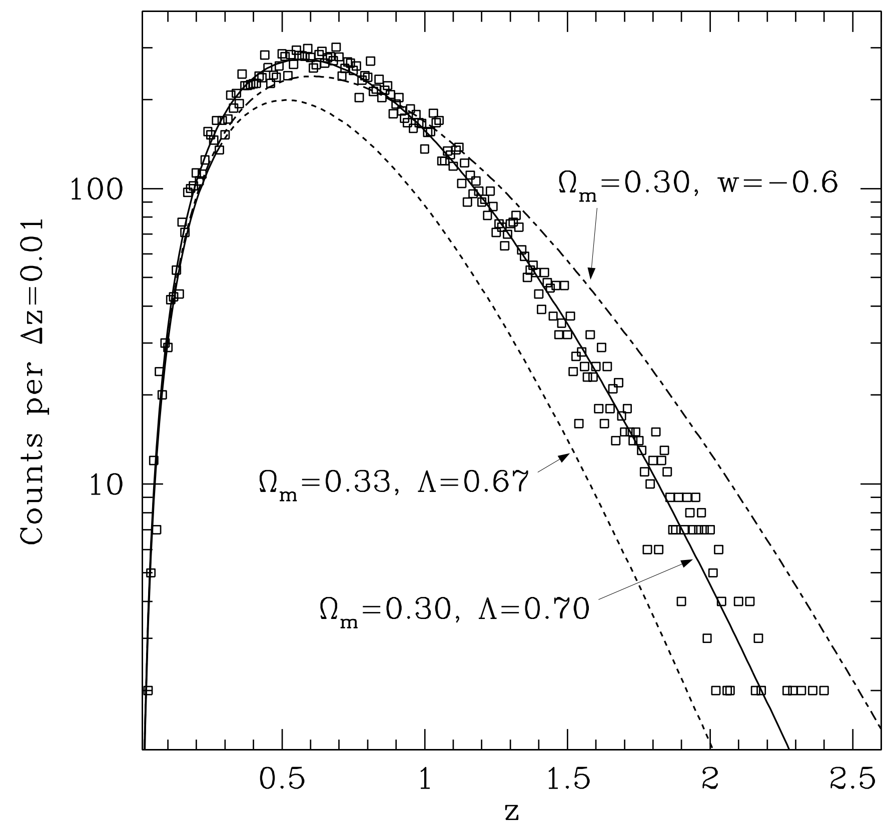

G. Holder

"Unbiased" Cluster Detection via the SZE

- "Unbiased" = mass-limited
- Effect is intrinsically redshift-independent: $\Delta T/T$ depends only on cluster properties, ΔT and T experience same redshift
- Standard argument: Integrated signal provides largely *z*-independent mass limit (Barbosa *et al*, Holder *et al*, etc.)

cluster mass

$$S_{tot} = \frac{2k_B^2\nu^2 g(x)\sigma_T T_{CMB}}{m_e c^4 d_A(z)^2} \langle T_e \rangle_n \frac{M_{200} f_{ICM}}{\mu_e m_p}$$

weak *z*-dependence of ang. diam. distance

- Integrate $n_e T_e$ over cluster face
- d_A^2 factor tends to reduce flux as z increases ($1/r^2$ law)
- But for a given mass, a cluster at high redshift has smaller *R* and hence higher *T*
- These two effects approximately cancel

“Unbiased” Cluster Detection via the SZE

- Holder, Mohr, et al (2000) modeled the mass limit of an interferometric SZE survey using simulations of cluster growth
- Simulations bear out expectation of weak z-dependence of mass limit
- v. different selection function from optical/x-ray surveys
- For any survey, careful modeling will be required to determine this precisely, understand uncertainties

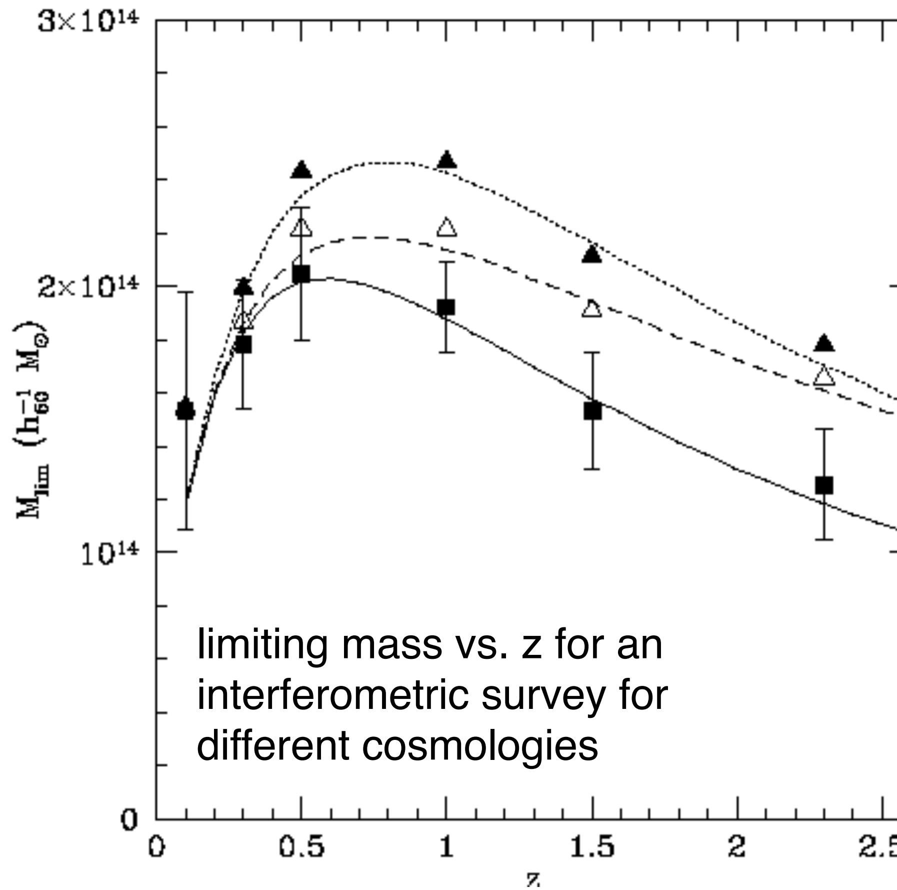

Holder *et al*, Ap. J., 544:629 (2000)

For the Near Term: High-ℓ SZ Anisotropy

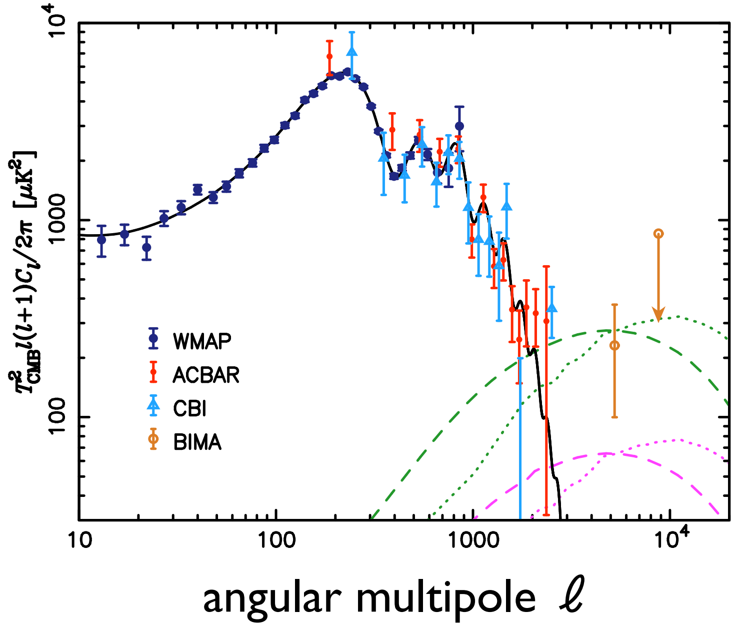

Readhead *et al* 2004, modified

- In the absence of cluster detections and redshifts, use anisotropy power spectrum to describe effect
- Tentative detection at high-ℓ by CBI, ACBAR, BIMA,

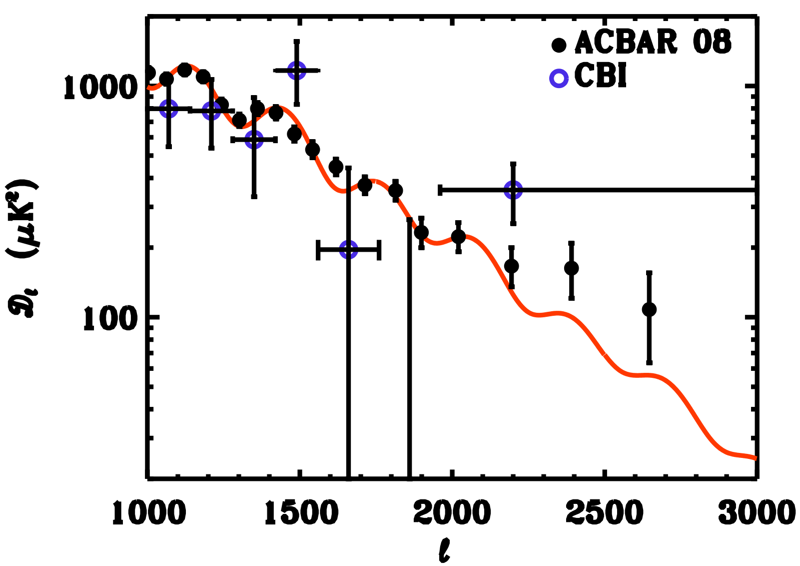

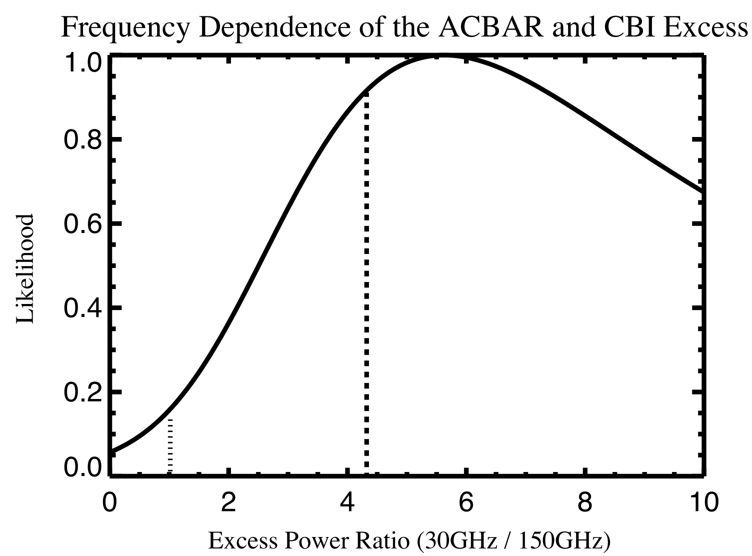

Reichardt *et al* 2008, modified

The High-ℓ Excess

- The high-ℓ excess seen by ACBAR, CBI, and BIMA is not entirely consistent with a SZ anisotropy explanation
  - SZ anisotropy expected to scale as $\sigma_8 (\Omega_b h)^2$; constraint on high-ℓ excess yields constraint on σ_8
  - CMB primary anisotropy + LSS also yields constraint on σ_8
  - ACBAR + WMAP3 primary PS + LSS $\rightarrow$ σ_8 = 0.81-0.85 +/- 0.03
  - ACBAR + CBI excess interpreted as SZ $\rightarrow$ σ_8 = 0.95 +/- 0.04
  - Dawson et al (2006) BIMA point: 220 +/- 130 μK_{CMB}^2 at 30 GHz $\rightarrow$ 55 +/- 33 μK_{CMB}^2 at 150 GHz vs. < 10 μK_{CMB}^2 for σ_8 = 0.80
  - ACBAR + WMAP3 can be reasonably interpreted as σ_8 ~ 0.80 SZ + unidentified point sources
  - Need better data!

Reichardt *et al* 2008, modified

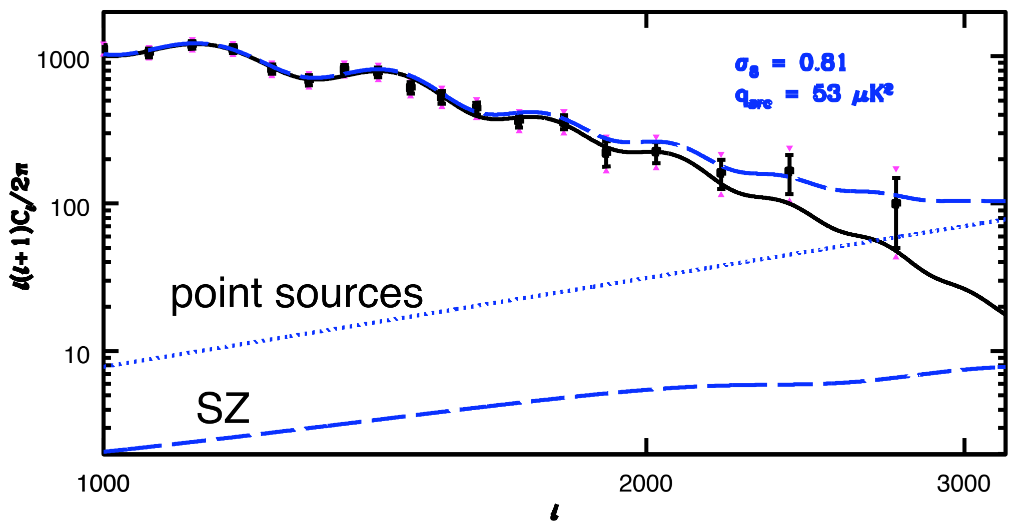

SZ Anisotropy: RJ Interferometers

- Experiments:
  - Sunyaev-Zeldovich Array: Carlstrom et al at CARMA site, 8 x 3.5 m dishes at 26-36 GHz and 85-115 GHz + CARMA
  - Arcminute Microkelvin Imager: MRAO, MRAO site, 10 x 3.7 m + 8 x 13 m, 12-18 GHz

SZ Anisotropy: MM-Wave Arrays

- mm-wave experiments (in order of existence and site quality)
  - Bolocam: 120 pixels at 150 GHz on 10.4 m CSO, Mauna Kea
  - APEX: 300 pixels at 150 GHz on 12 m ALMA prototype, ALMA site
  - ACT: 1000 pixels each at 150, 220, 275 GHz on 6-m off-axis az-scanning dish, Cerro Toco
  - SPT: 1000 pixels distributed across 90, 150, 220 GHz bands on 10-m off-axis dish, South Pole

Bolocam/CSO

APEX

ACT

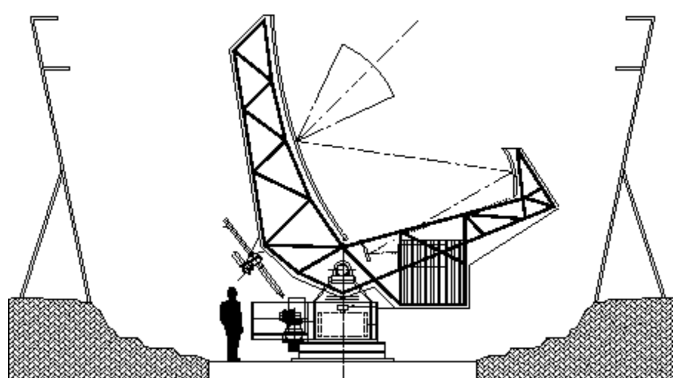

SPT

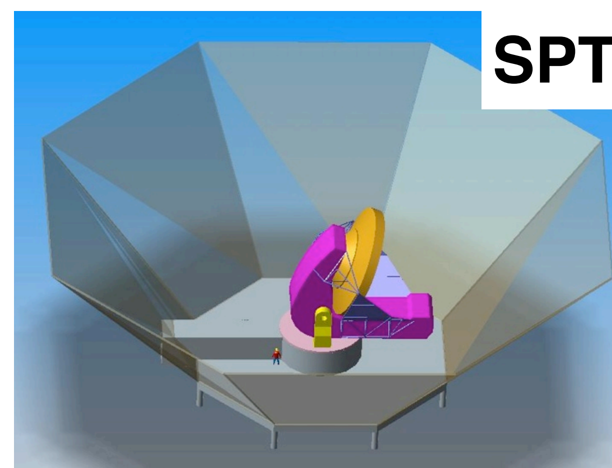

Bolocam Overview

- Observation bands:
  - 125-165 GHz: thermal SZ
  - 225-300 GHz: dusty sources
  - (217 GHz: kinetic SZ)
- 144-pixel spiderweb bolometer array operated at ~ 250 mK
- Array architecture:
  - Bolometers are bgnd-limited; increase sensitivity with pixel count (8' FOV)
  - Sky noise removal enabled by beam overlap through atmosphere
- At Caltech Submm Obs., 10-m on Mauna Kea

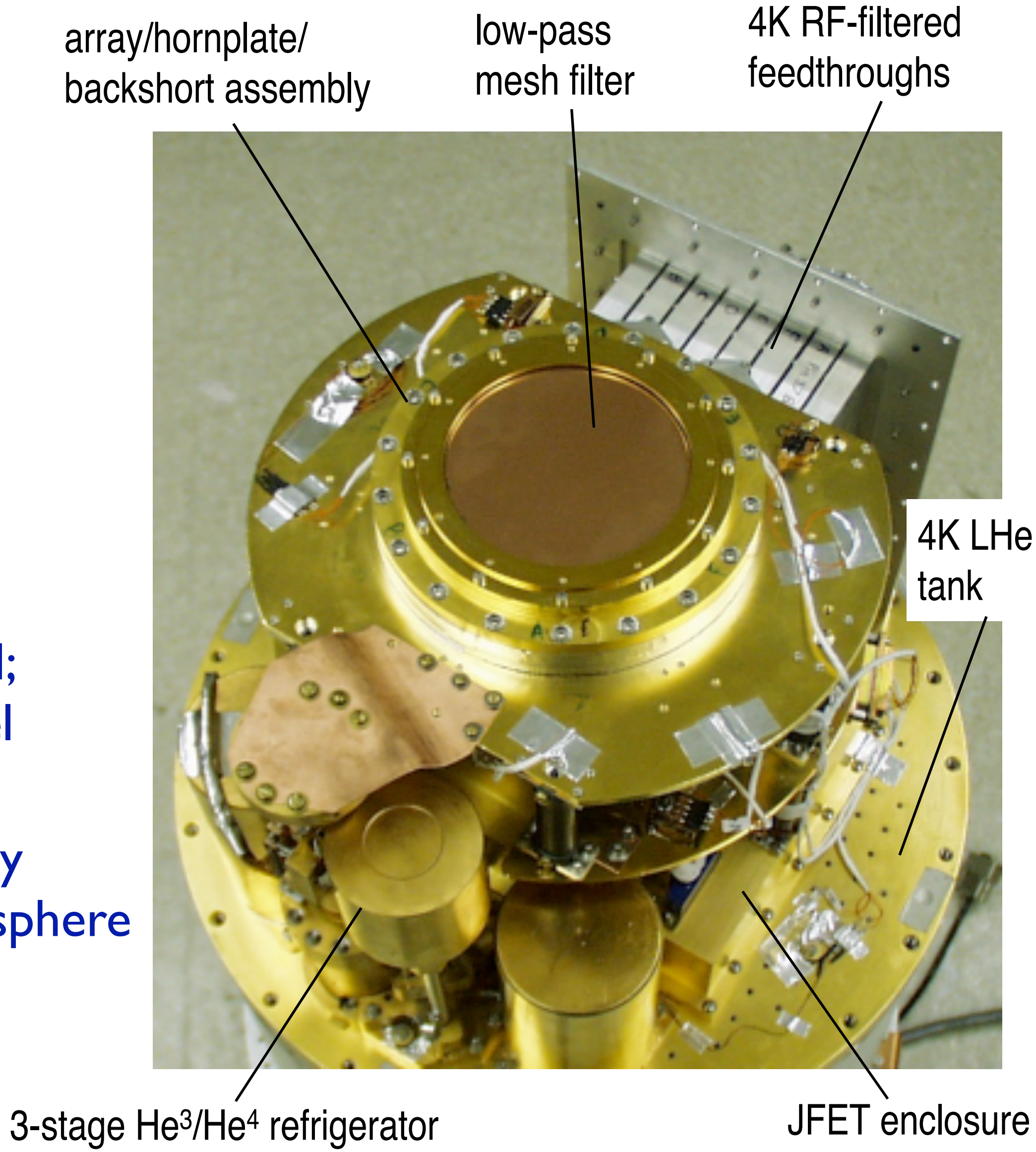

Instrument Team

- Caltech
  - (Mihail Amarie), (Samantha Edgington), Sunil Golwala, Andrew Lange, Philippe Rossinot, Jack Sayers
- JPL
  - Jamie Bock, (Alexey Goldin), Hien Nguyen, Fab team at MDL
- University of Colorado, Boulder
  - James Aguirre, Jason Glenn, (Ben Knowles), Glenn Laurent, Phil Maloney, James Schlaerth, (Patrick Stover)
- University of Wales, Cardiff
  - Peter Ade, Douglas Haig, Phil Mauskopf, Rob Tucker

PhD thesis Dec 2007,
has done bulk of analysis work

Bolometer Array

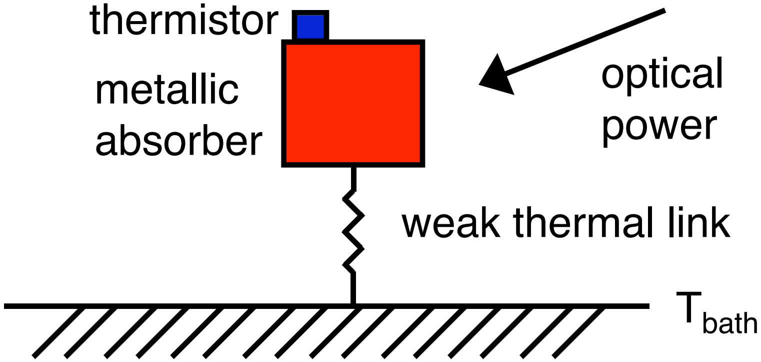

- 144 bolometers on single wafer: J. Bock, JPL/MDL
- 125 Å Au absorber on 1 μm SiN membrane, etched into "spider-web" to minimize C_{Au}, G
- NTD Ge thermistor senses T
- Array production nontrivial

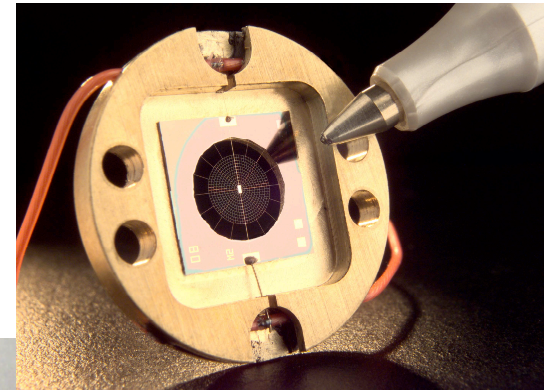
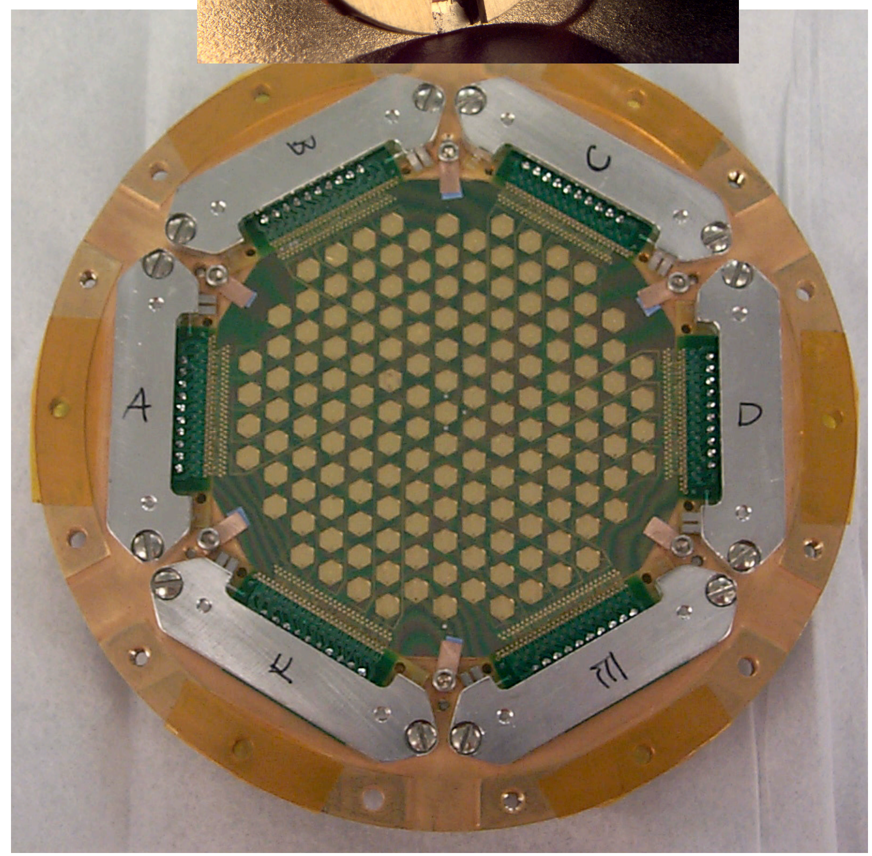

Optical Design

- Smooth-walled conical feedhorns define beams
- Horns coupled to integrating cavities via 2λ length of single-mode waveguide (defines lower edge of BP)
- Integrating cavities house bolos, yield > 90% efficiency and < 1% optical crosstalk
- Monolithic construction
  - single feedhorn plate
  - single backshort plate
- Backshort and hornplate can be exchanged easily
  ⇒ "easy" to change bands

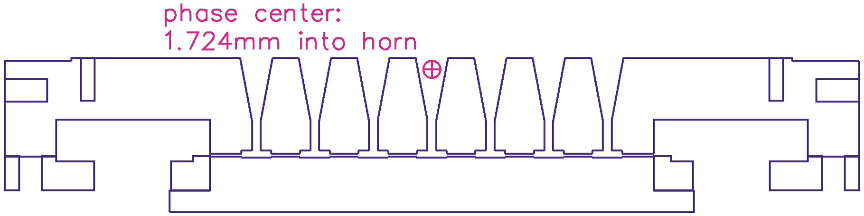

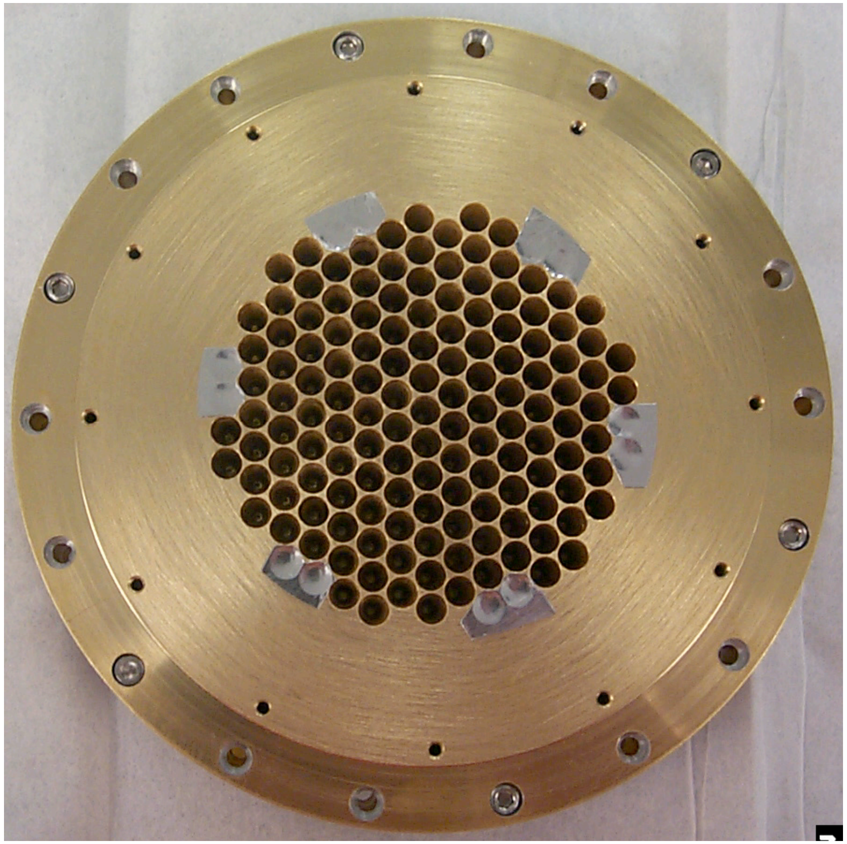

Optical Design

- Ellipsoidal tertiary and cold HDPE lens provide wide FOV (8') at F/3 plate scale
- 5 cold metal-mesh filters define high end of band while minimizing harmonics leaks
- Reflective IR blocker at 77K
- 4K Lyot stop defines illumination of primary (modulo diffr. blurring)

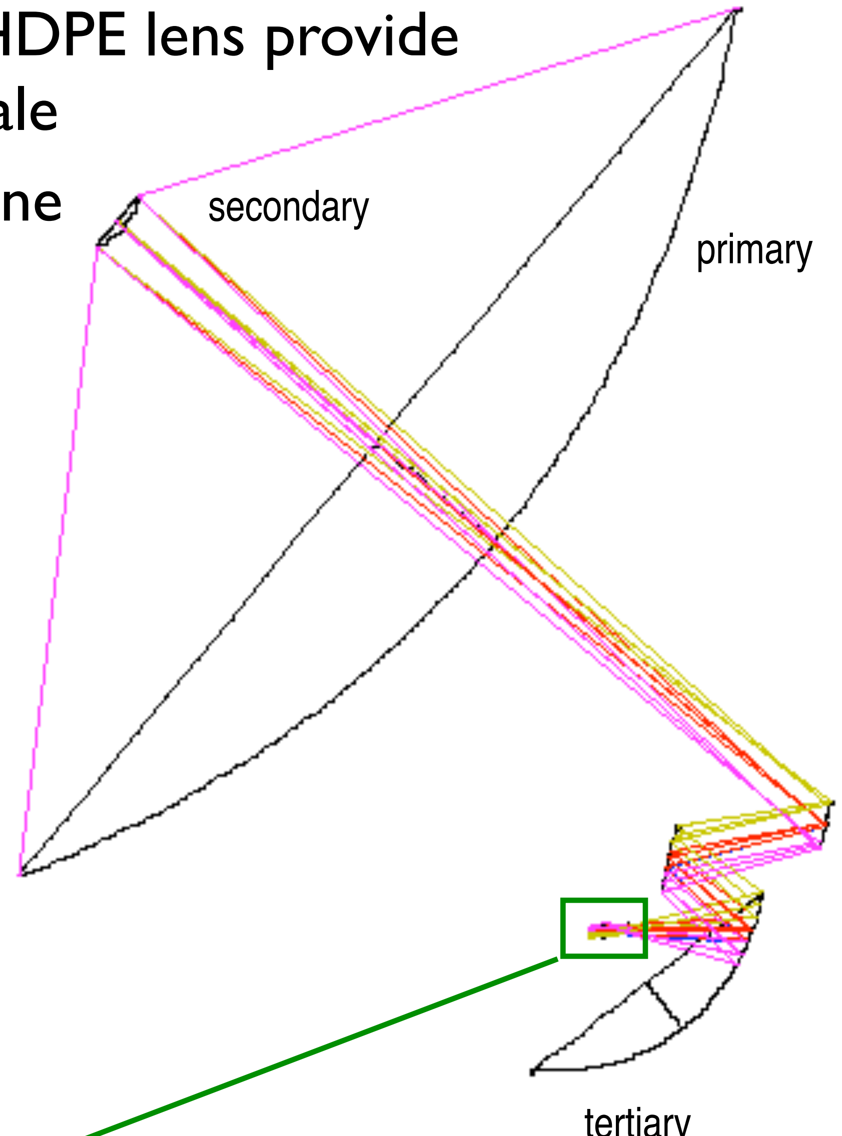

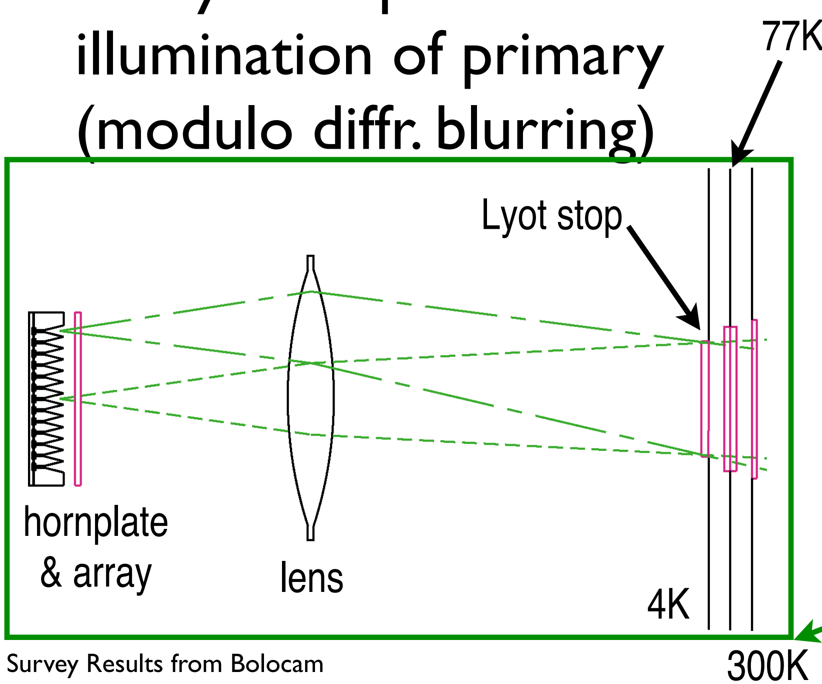

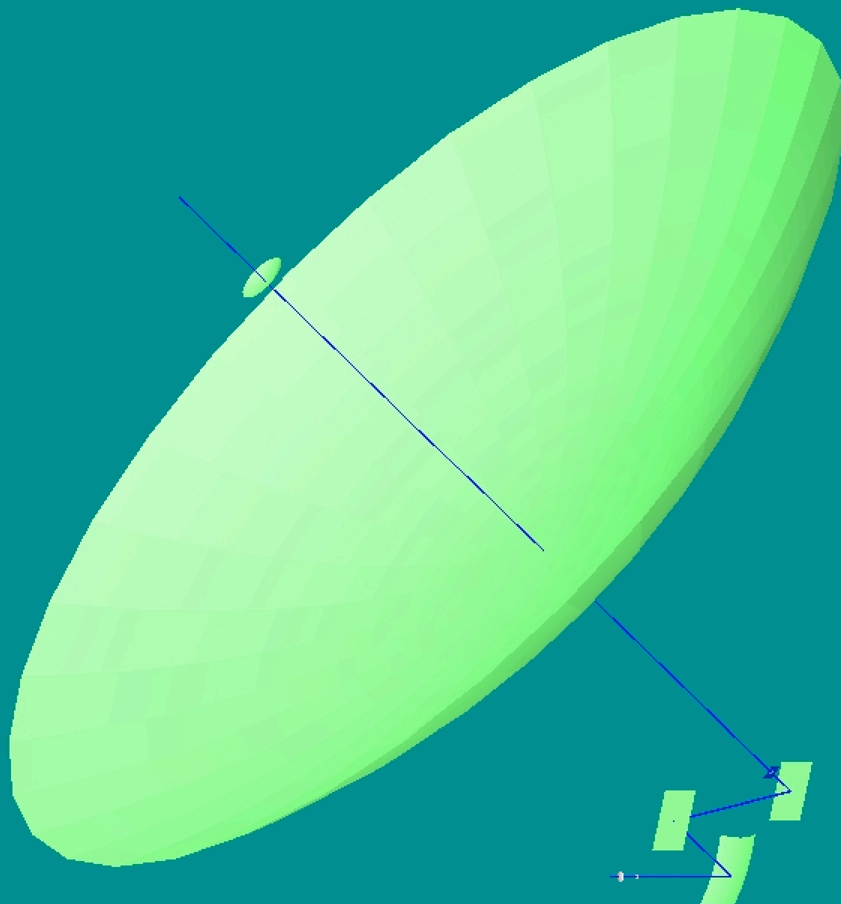

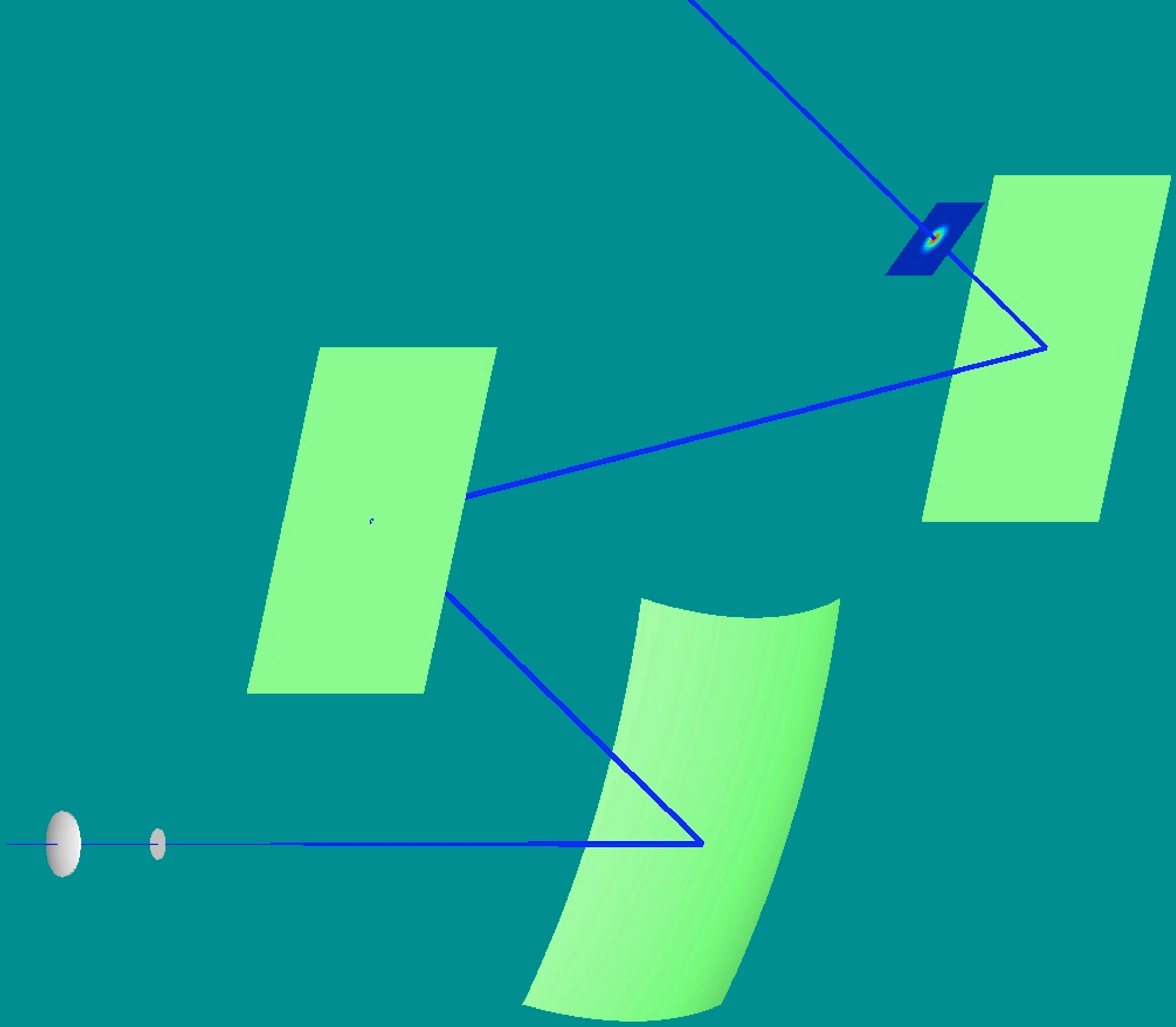

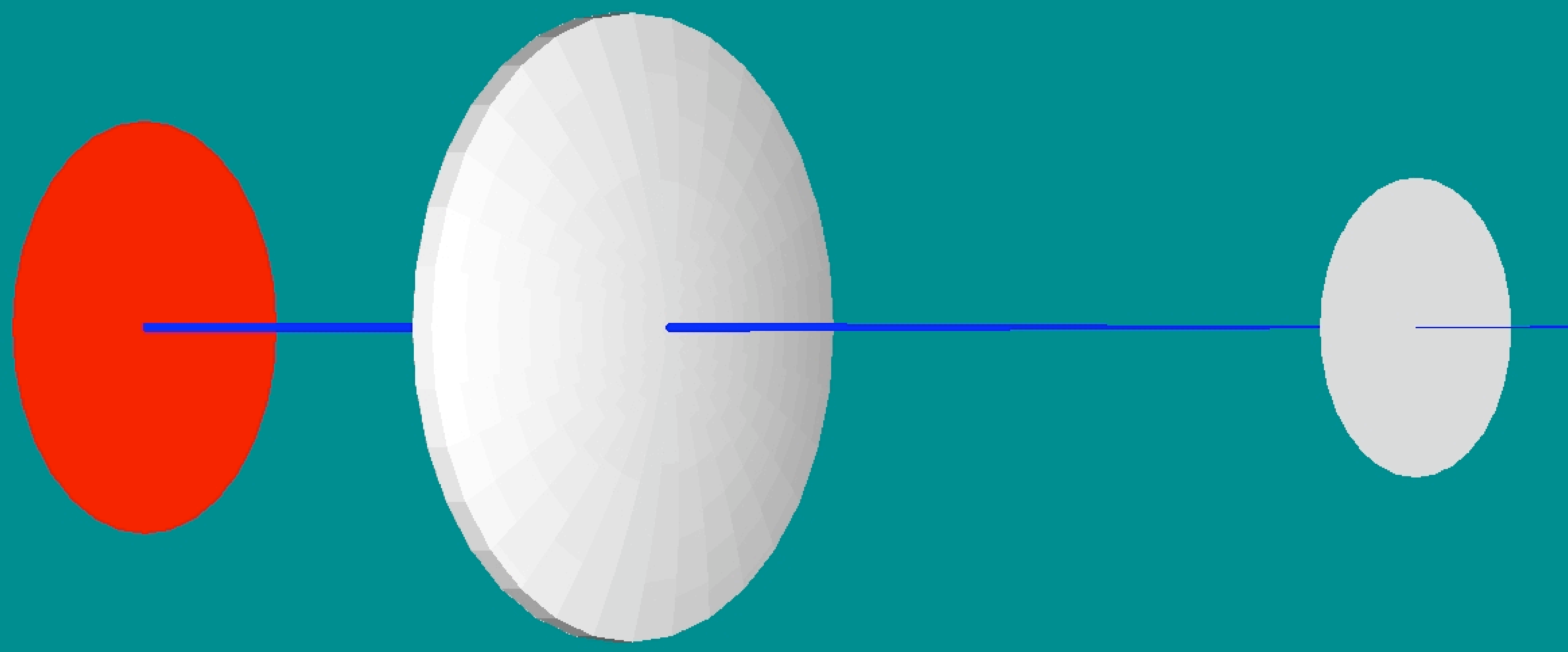

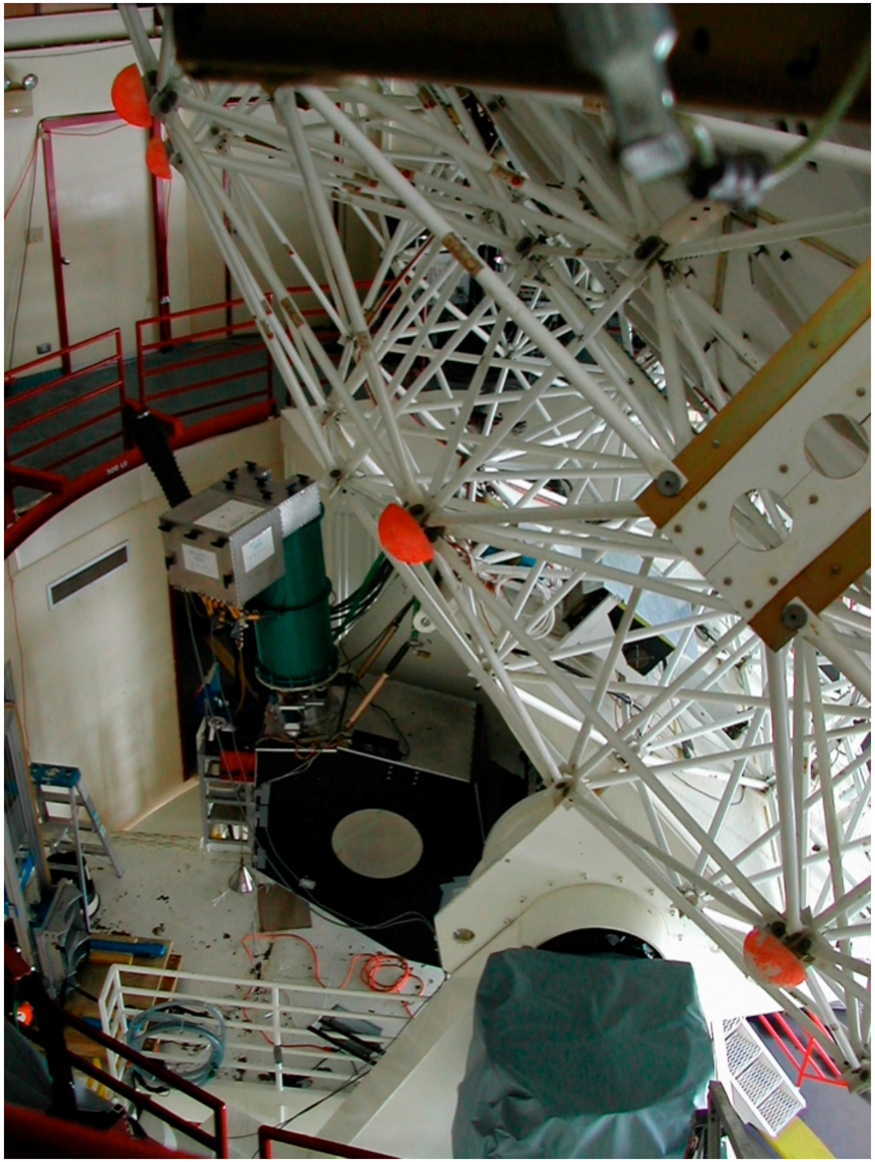

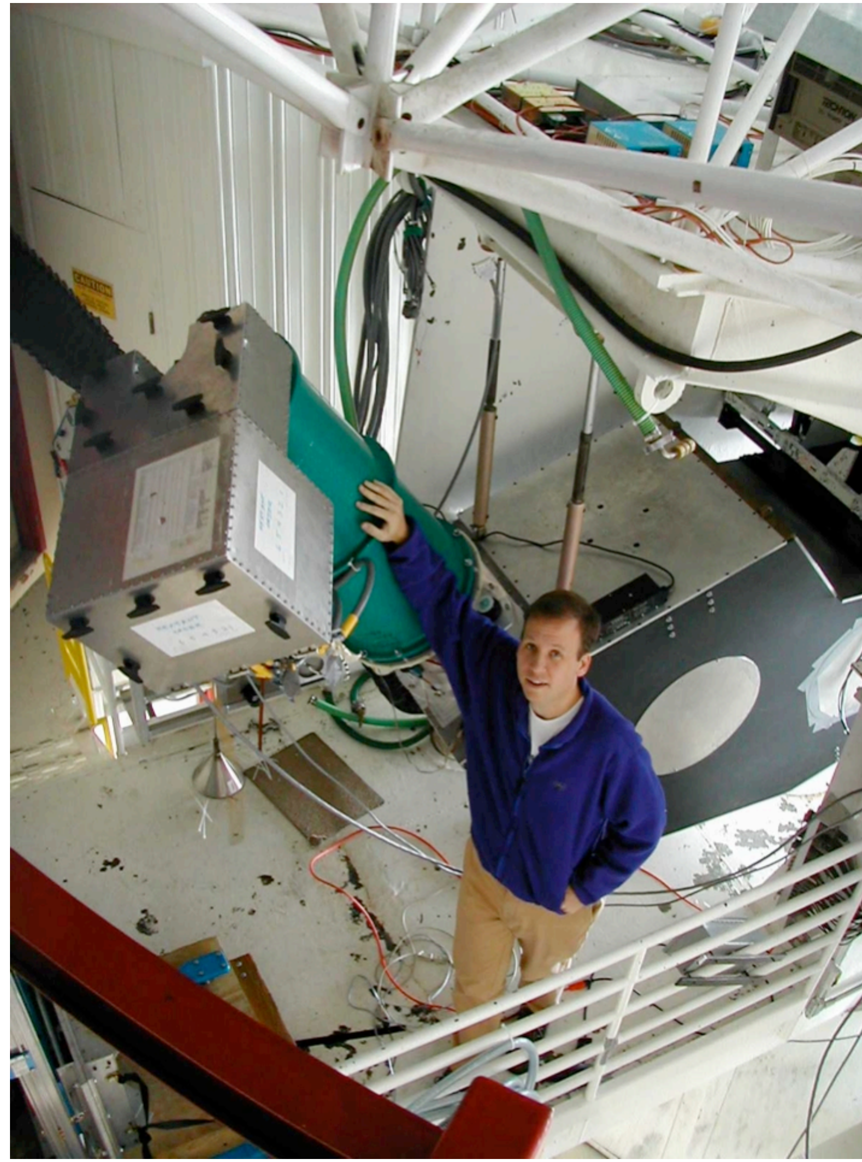

150 GHz Blind Sunyaev-Zeldovich Effect Survey

- 2 fields, each 0.5 deg^2
  - Wanted low dust emission, good X-ray and optical coverage in case clusters were found
  - SDS1 (aka SXDS): Subaru deep survey field
    - 400 ksec XMM-EPIC integration time
    - OIR coverage by surveys on Subaru, CFHT Legacy, UKIRT, Spitzer SWIRE Legacy survey
    - 12 μJy VLA coverage
    - SCUBA SHADES and BLAST field
    - 1.2 MJy/ster 100 μm dust emission, among the lowest in the sky
  - Lynx: not so well complemented
    - 150 ksec XMM-EPIC
    - imaging of small portions containing low-mass clusters
    - 1.3 MJy/ster 100 μm emission, also pretty good
- ~ 40 nights of telescope time in fall 2003

150 GHz Blind Sunyaev-Zeldovich Effect Survey

- Observing Strategy
  - Spend half the night on each field, 6-8 hrs each per night
  - Raster over each field along the RA and dec directions
    - Drift scan would be less prone to scan-synchronous pickup, but sky noise pushes one to active scanning to move signal to higher temporal frequency
    - Active az-only scans produce inefficient coverage pattern due to sky rotation
    - Good belief that array would allow subtraction of elevation dependent signal

after sky noise removal!

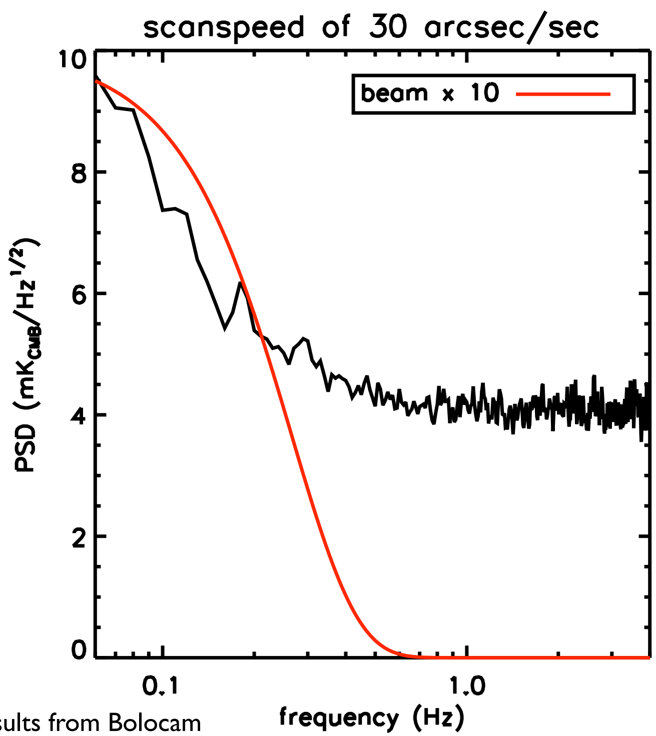

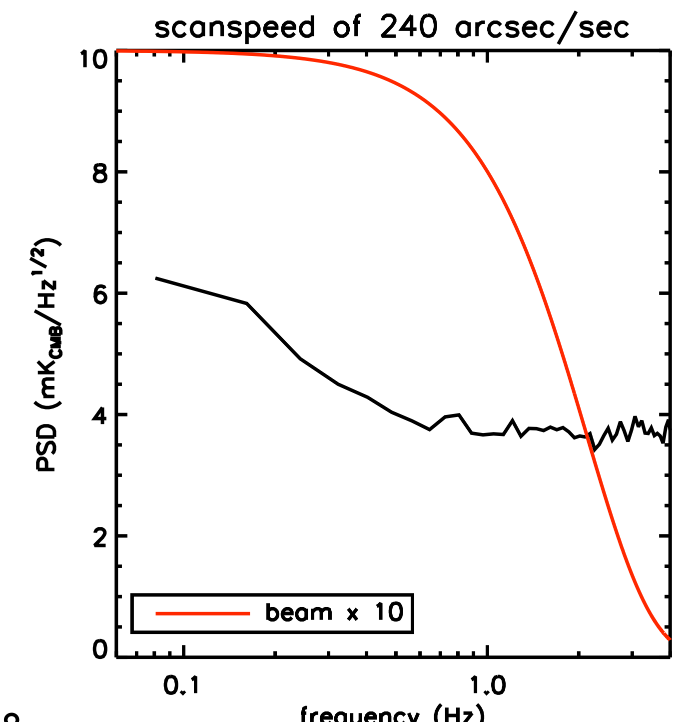

150 GHz Blind Sunyaev-Zeldovich Effect Survey

- Observing Strategy
  - Data broken up into 8-minute-long "observations"
    - Each observation covers the entire field in one scan mode with 8-9% rms coverage variations (4-5% noise variations)
    - Alternate RA and dec scans
    - 3 sets of offsets perpendicular to scan direction to smooth out coverage
    - Final maps have 1.5% coverage variations

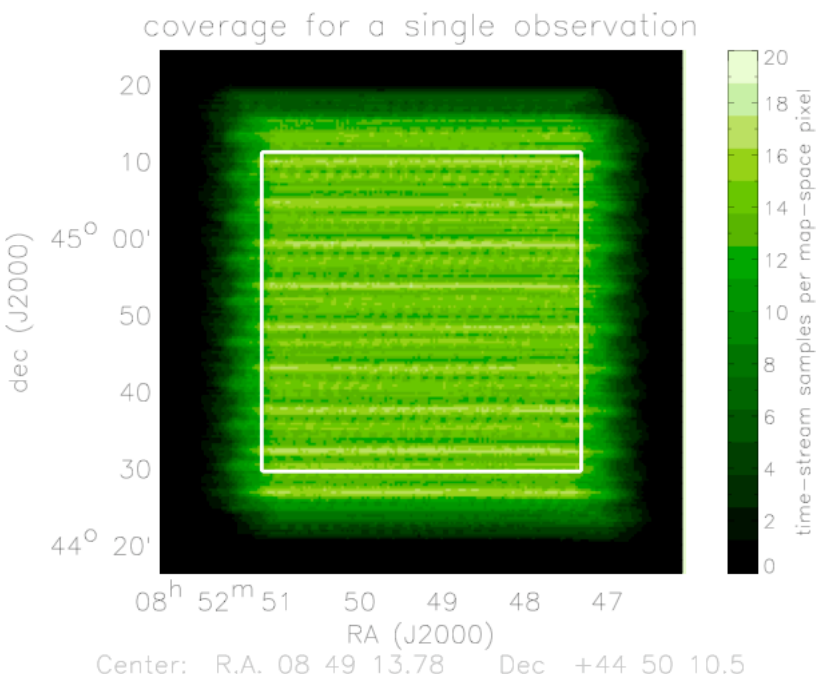

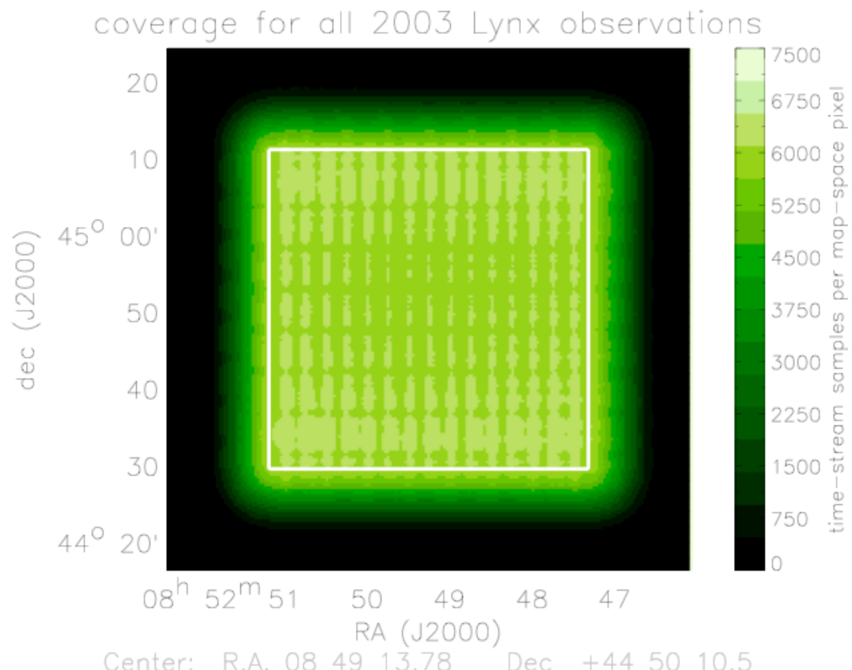

Observing Conditions: Loading and Opacity

- To first order, the atmosphere!
- Median conditions: 1.75 mm of water between the instrument and the CMB!
- Atmospheric optical depth:
  - 150 GHz: $\tau \sim 0.05$
  - 275 GHz: $\tau \sim 0.13$

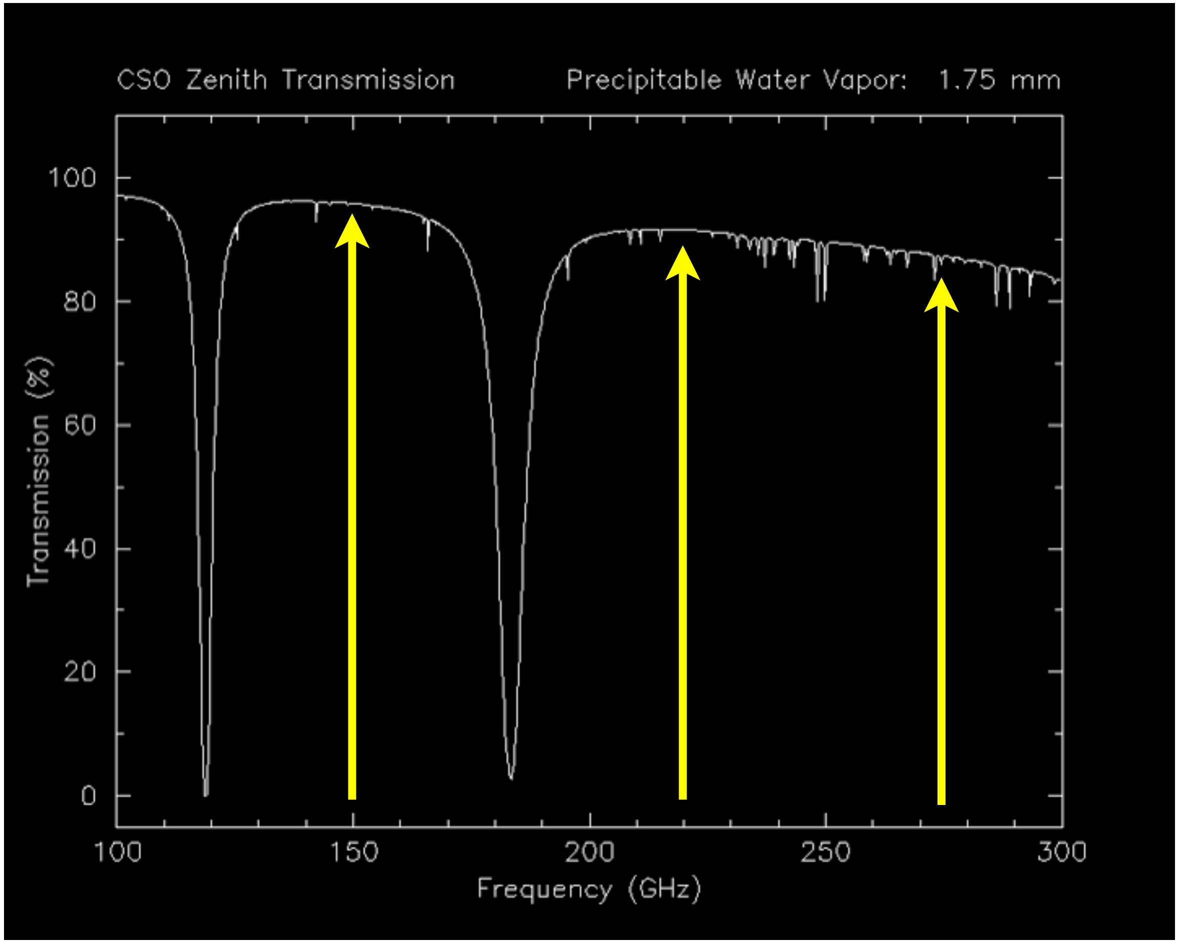

- Photon Poisson and Bose noise from the emitted power

Observing Conditions: Sky Noise

- water vapor w/scale height of ~ 2 km
  - near condensation point, so clumpy
  - strong dipole moment ⇒ rotation couples well to mm-waves
- liquid water: same modes, but much less efficient, constrained by inter-molecule forces
- ice: rotation is prevented
- Water vapor present as turbulent screen entrained in wind

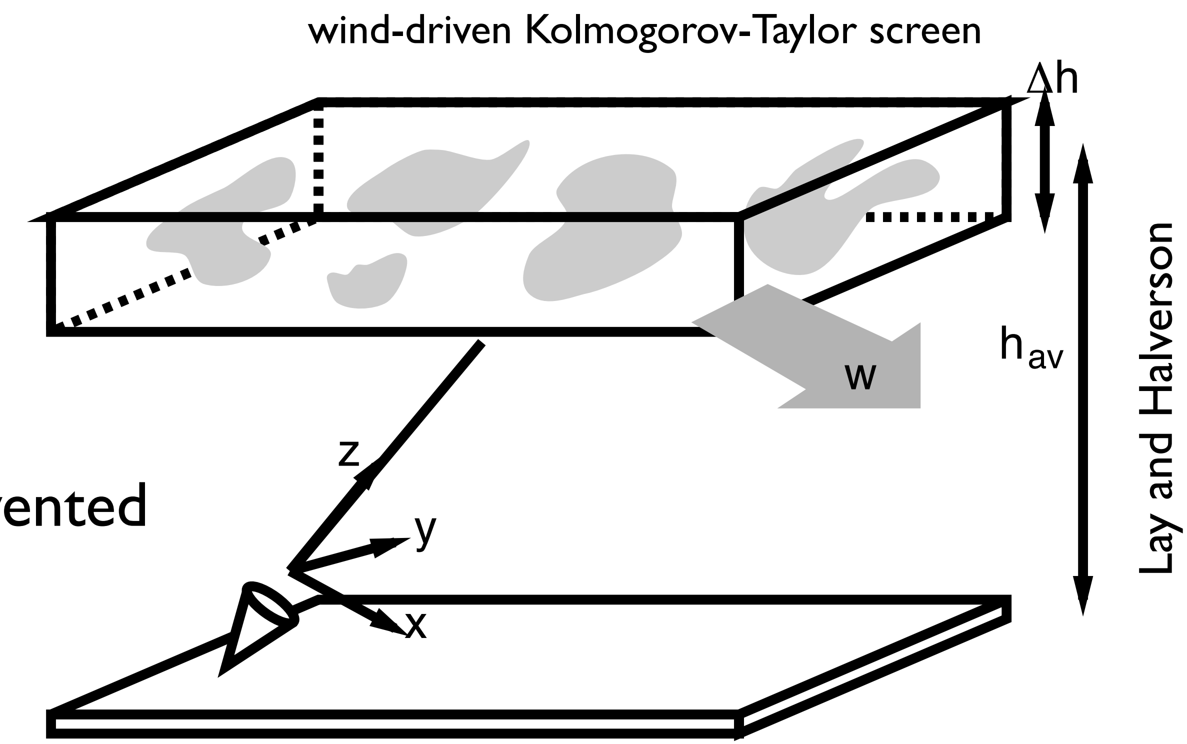

Observing Conditions: Sky Noise

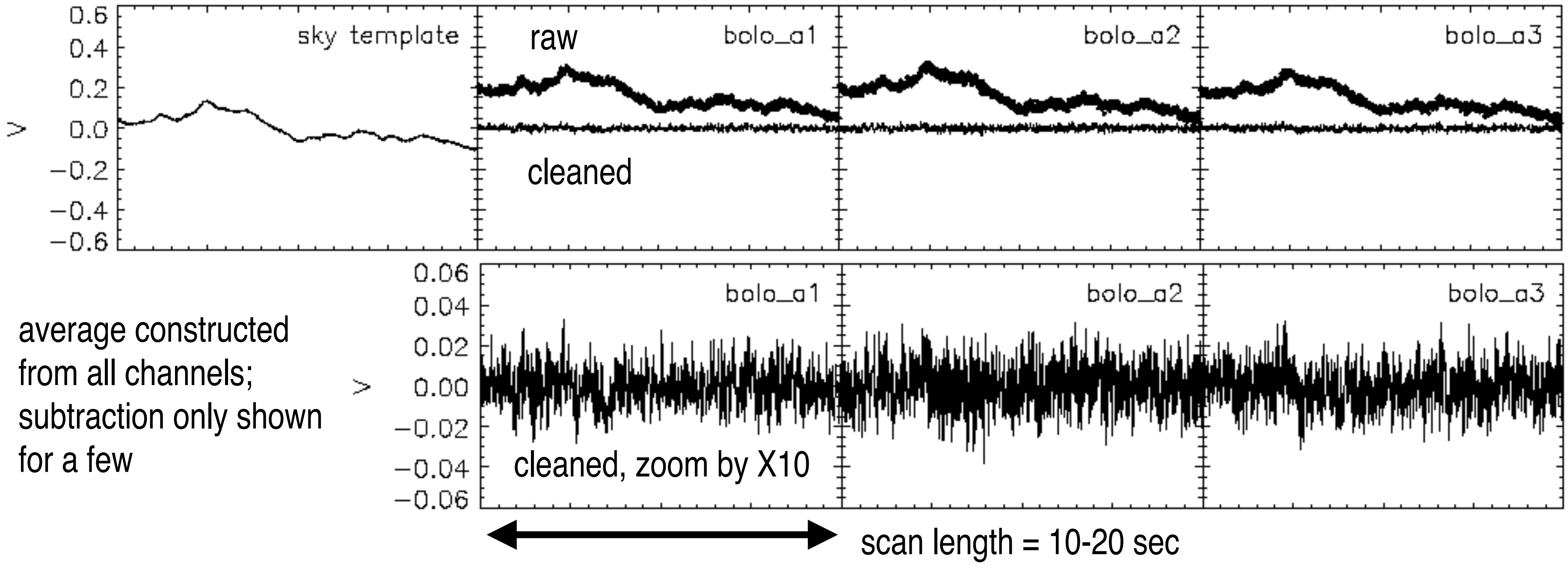

- Sky noise = fluctuations in emission from water vapor in atmosphere due to wind-driven turbulent screen
- Overlap of beams through atmosphere ensures it is mostly common signal
- A simple average removal takes out >90% of sky noise

Autocorrelation Function of Sky Noise

- See expected power-law autocorrelation function of sky noise as a function of pixel separation (structure function)
- Correlation length varies; large corr. length → good sky subtraction
- Excess correlation visible at small separations, worst when sky noise is poor. Consistent with spread of Airy function.

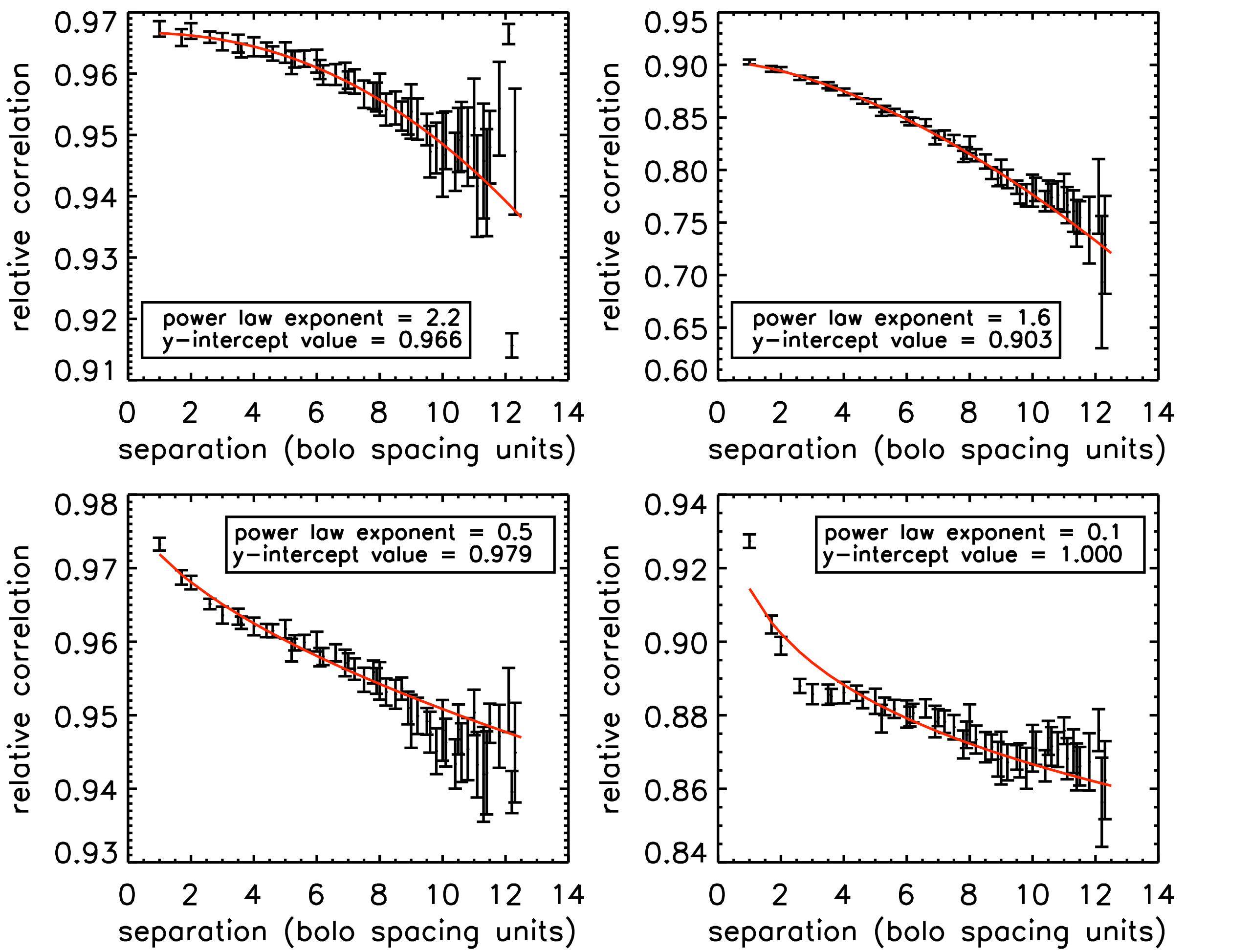

Sky Noise

- Average removal leaves significant noise above fundamental photon + instrument noise
- First, attempt to model as wind-driven screen: get sensible wind speeds, but no improvement

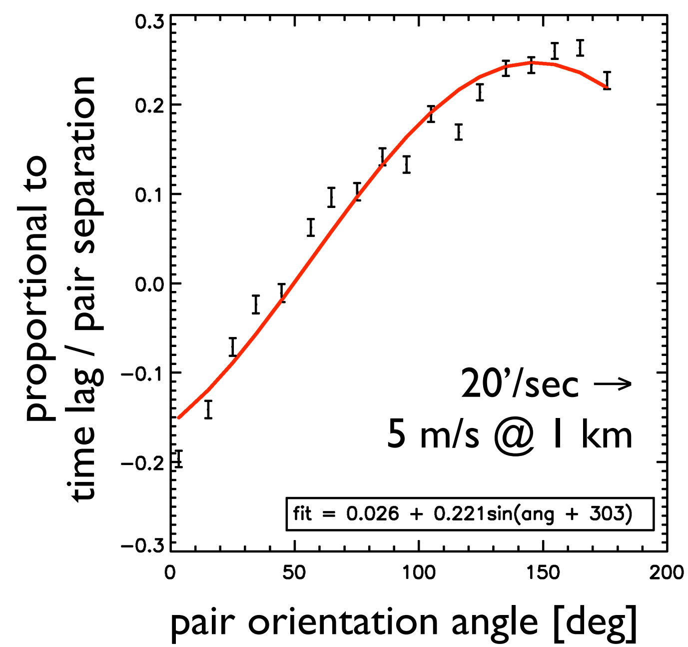

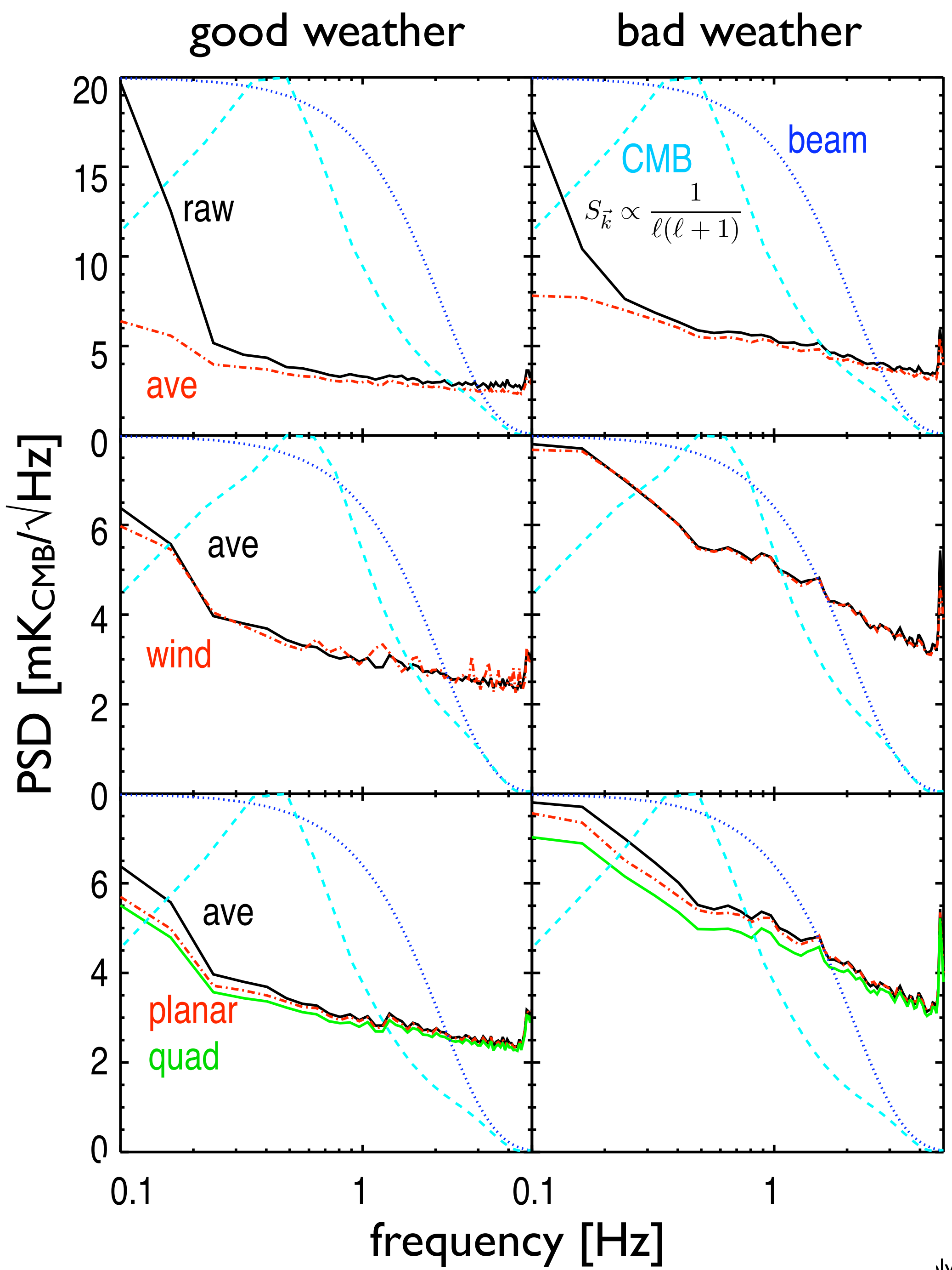

Sky Noise

- Think a bit harder:
  - typical wind speed: 10 m/s @1km = 35'/sec
  - telescope scan speed = 4'/sec « wind speed so neglect telescope motion
  - noise is below 0.5 Hz; T = 2 sec, w = 35'/sec get θ = w T > 1 deg » 8' FOV

    ⇒ on scale of array, see only polynomial-like portion of mode
  - fit for average, plane, or quadratic across FOV

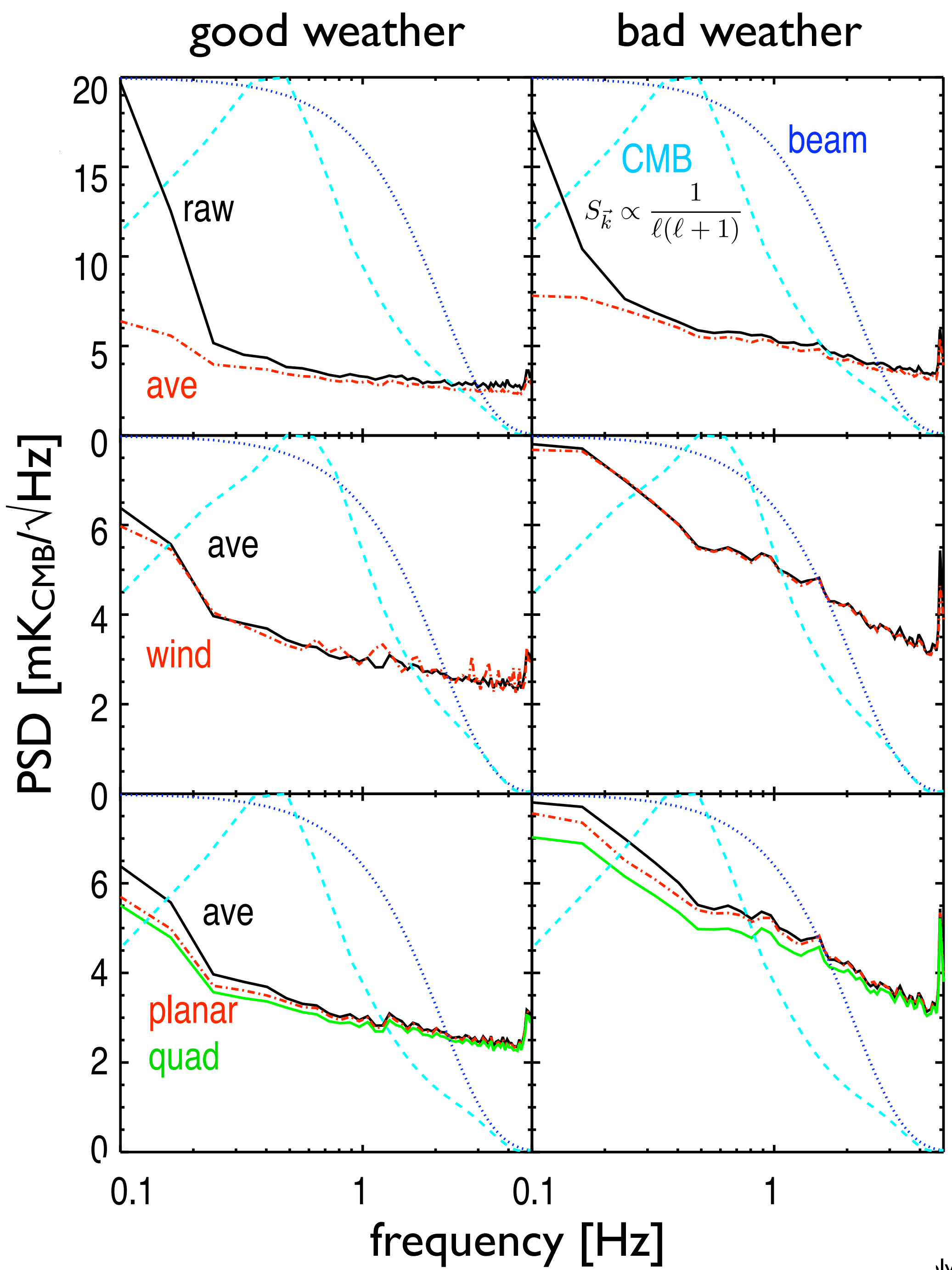

Map-Space PSDs

- Subtraction methods similar in timestream, differ in map space
  - (Naive mapmaker; see below for more sophisticated version)
  - Residual correlations manifest as low-ℓ noise
  - More aggressive methods reduce residual correlations among bolometers

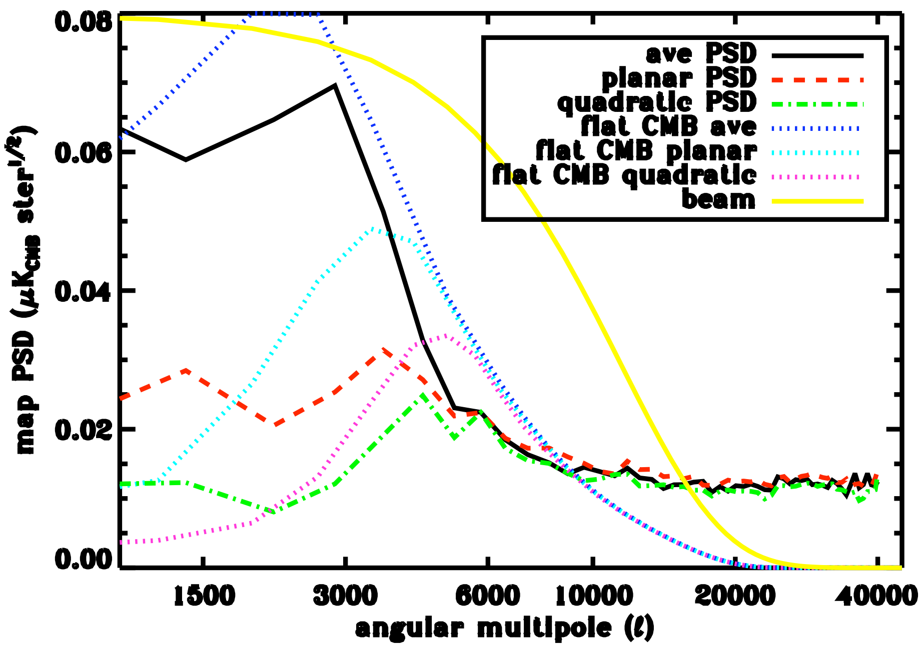

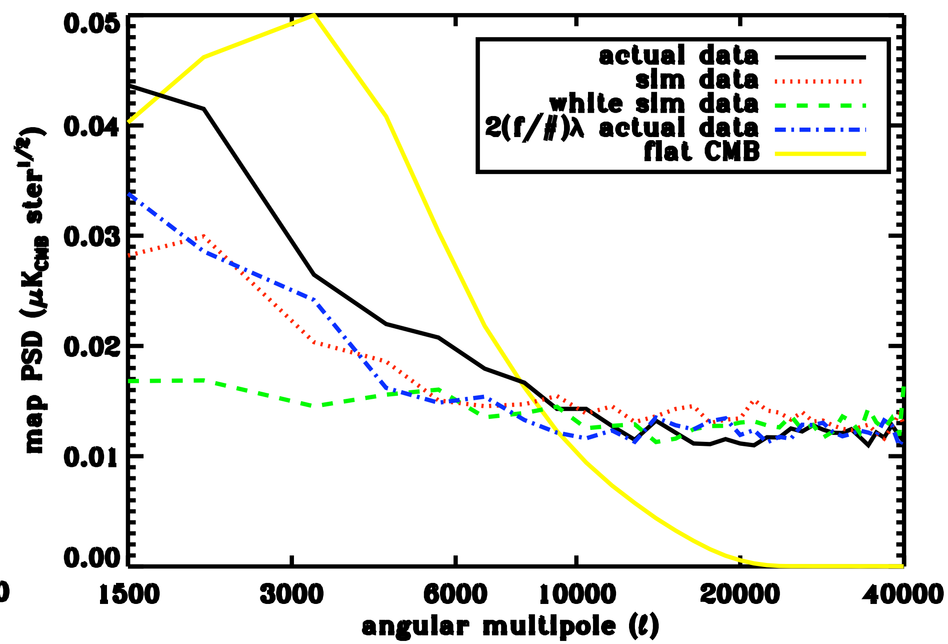

(transfer functions not deconvolved)

Map-Space PSDs

data type	PSD spectrum	PS amplitude uncertainty
actual/36 spaced detectors	data	550 μK_{CMB}^2
actual/115 detectors	data	270 μK_{CMB}^2
sim/115 detectors	data	170 μK_{CMB}^2
sim/115 detectors	instrument, white	100 μK_{CMB}^2

consistent with √N

inconsistent with √N

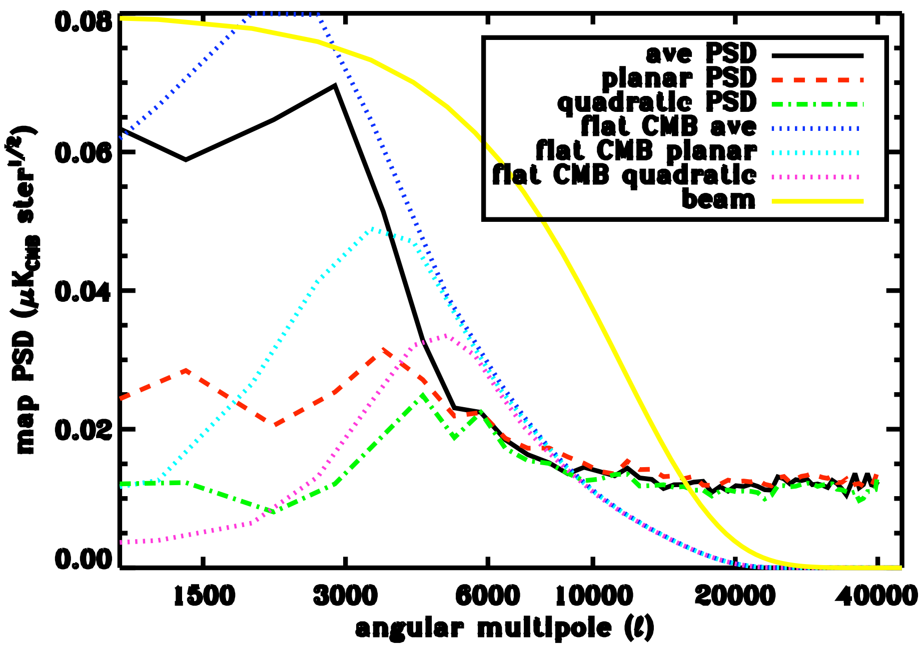

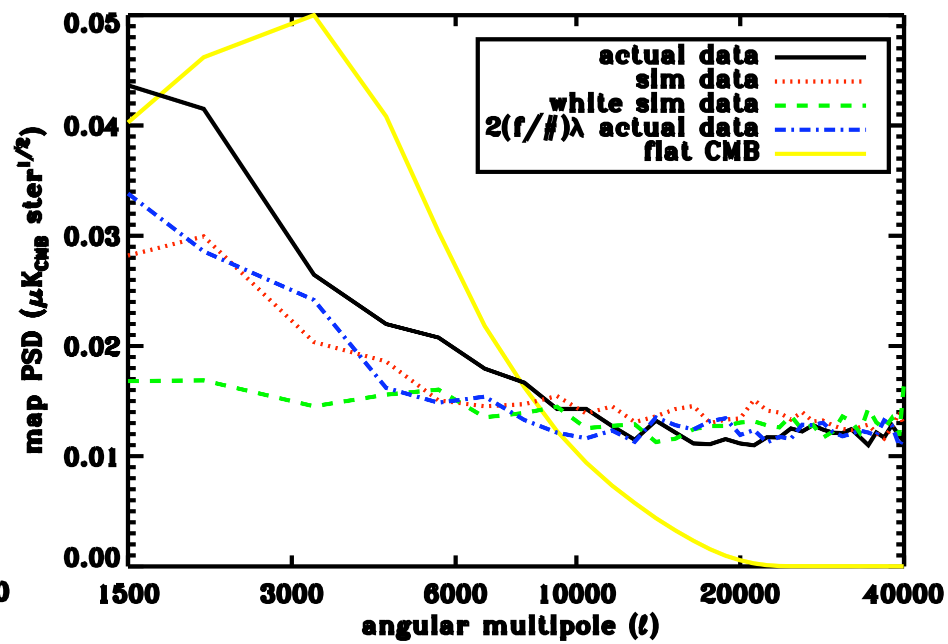

(transfer functions not deconvolved)

Residual Spatial Correlations

- There is residual correlation between nearby bolometers post sky-subtraction
  - lower in better weather
  - excess correlation at sub-(f/#)λ separations
    - one bolo separation = 0.7 (f/#)λ
    - Need to go out to *r* ~ 2 (f/#)λ before residual correlations look flat with *r*
    - Effective number of pixels drops by a large factor:
      degradation in μK_{CMB}^2
      ~ degradation in number of pixels

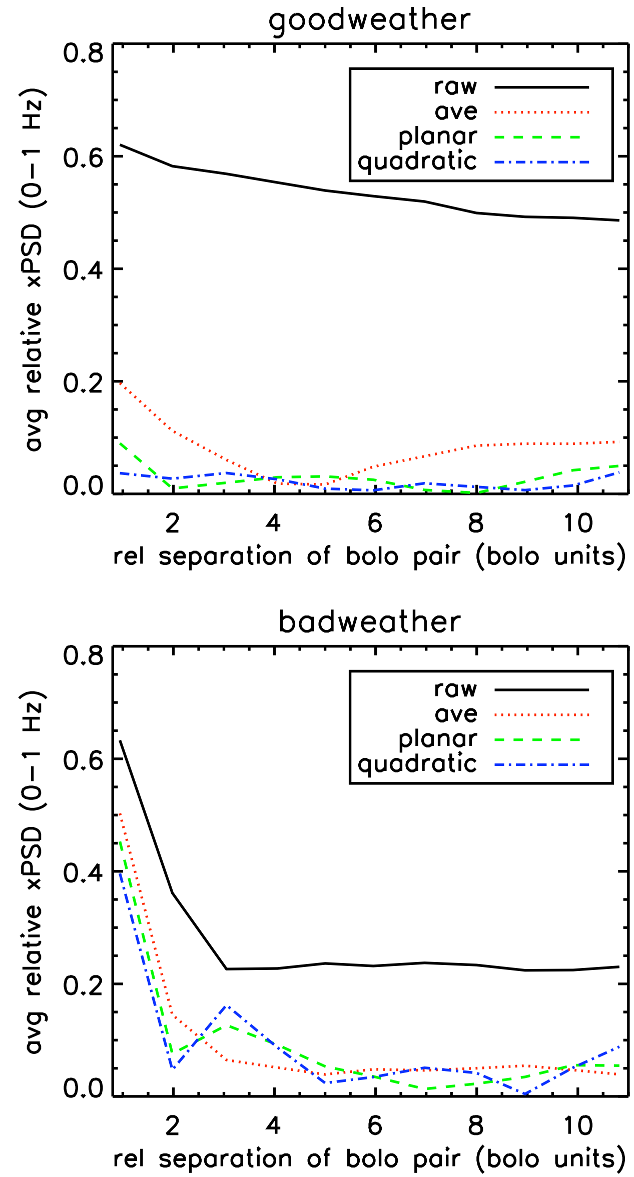

Map-Space PSDs

good weather
RA scan

$\ell = 2\pi\nu$

bad weather
dec scan

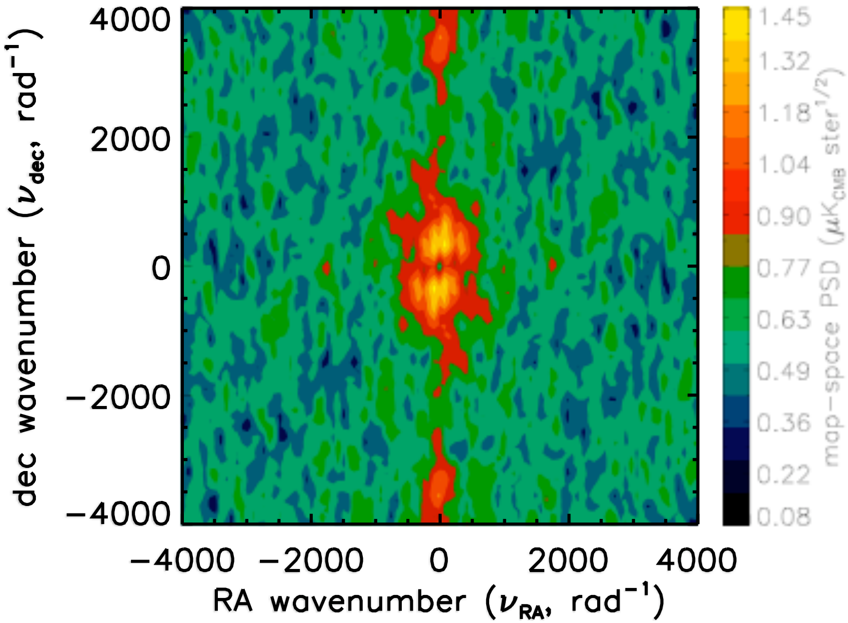

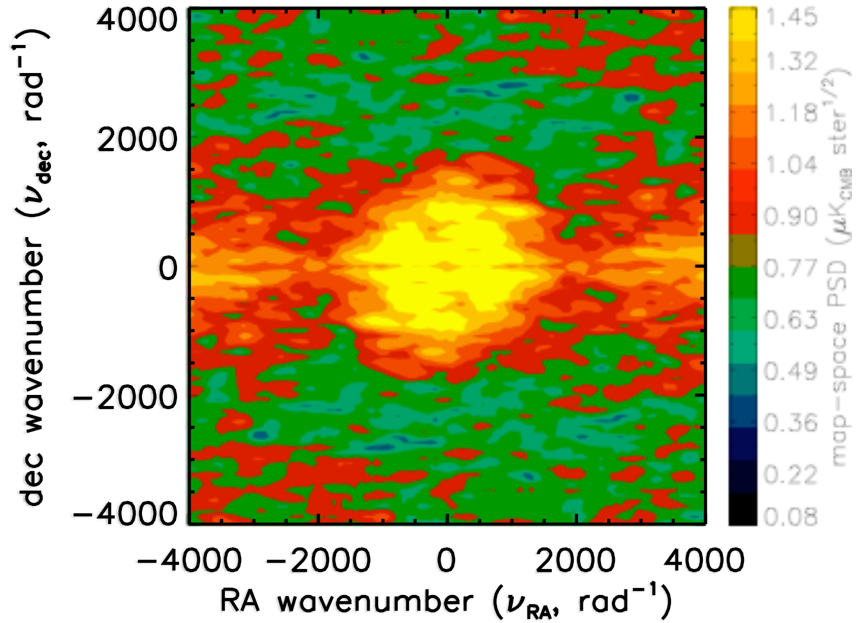

- Scan type is evident in map-space PSDs
- Variations in low-frequency noise clear
- Very gaussian except at small deviations

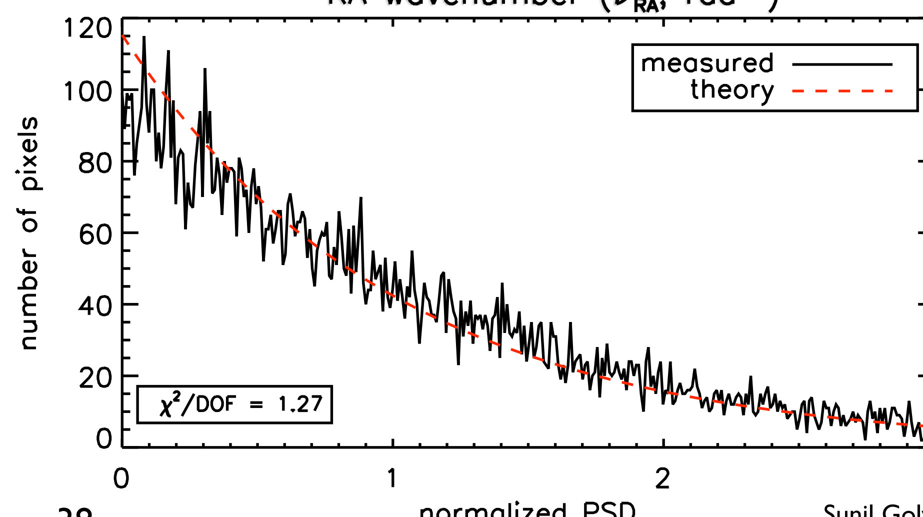

Sky Noise Removal Window Function

- Sky noise removal via correlation analysis reduces sensitivity to signal on scales ≳ 8' FOV. λ_θ= 8' ⇒ ℓ = 2700
- More aggressive sky noise removal also removes more signal
- Measure transfer function of sky noise removal by inserting simulated CMB (flat in $\ell(\ell+1)C_\ell$) into timestreams and measuring attenuation at output map as a function of ℓ
- Transfer function is independent of signal amplitude at signal levels of interest
- $BW_{eff} = \Delta \log(\ell)$

$$\mathrm{BW}_{eff} = \int_{\vec{\nu}} d\vec{\nu} S_{\vec{\nu}} W_{\vec{\nu}} B_{\vec{\nu}}$$

$$S_{\vec{\nu}} \propto \frac{1}{\ell(\ell+1)}$$

$$\ell = 2\pi\nu$$

$$W_{\vec{\nu}} B_{\vec{\nu}}$$

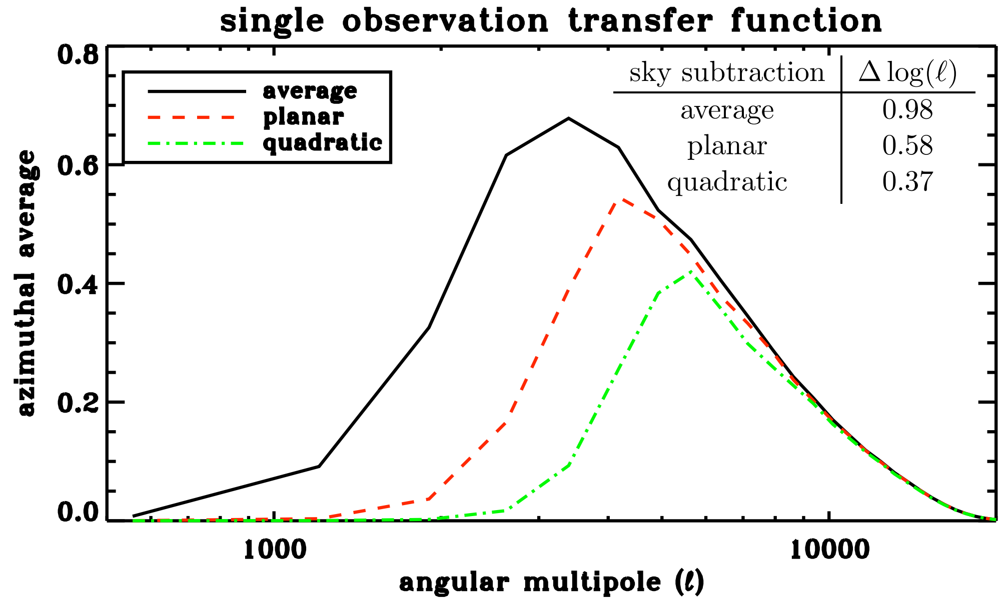

Single-Observation Transfer Functions

- Asymmetry from scan pattern evident

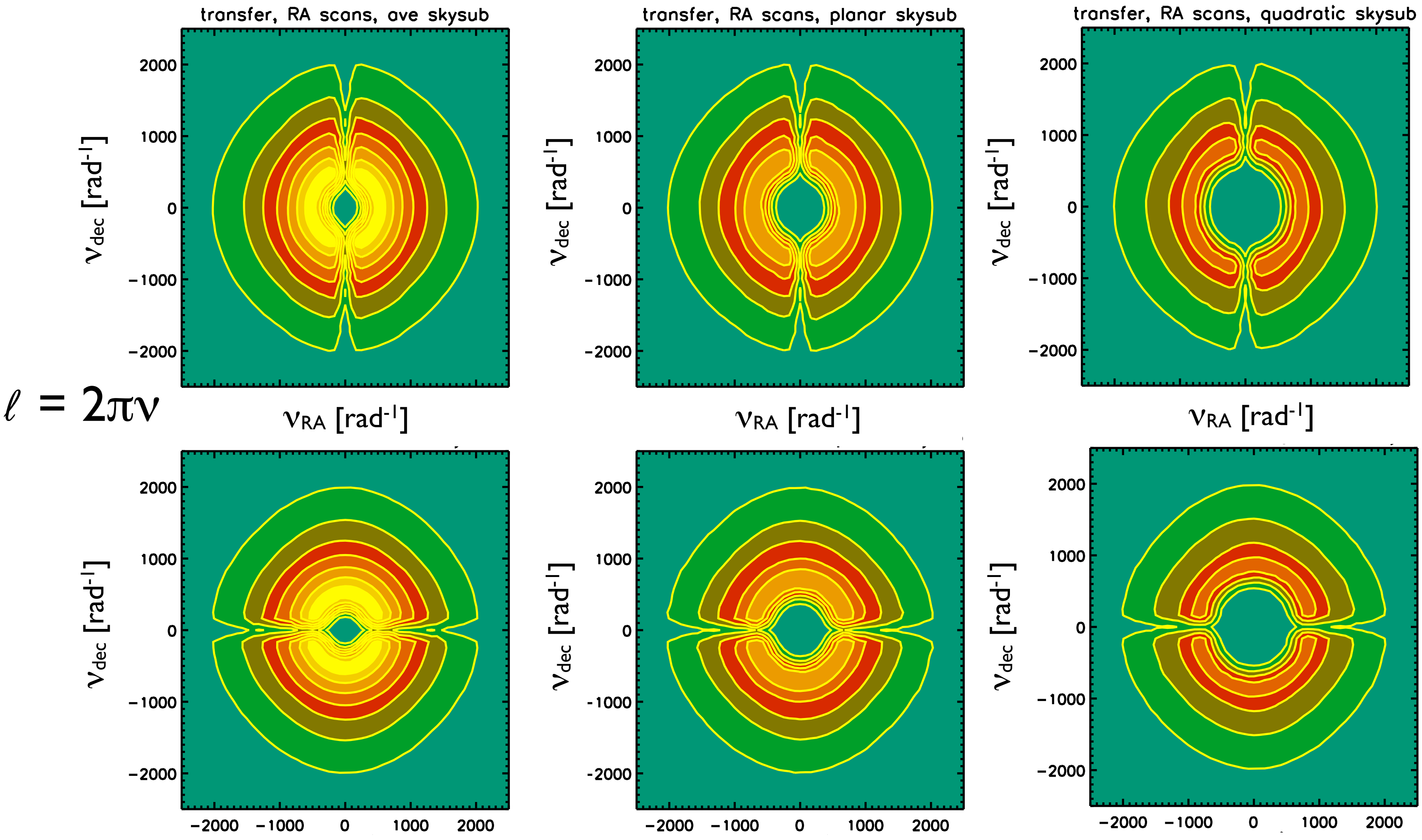

Mapmaking

- Standard Max Likelihood mapmaking is difficult for us

$$\chi^2 = (\vec{d} - \mathbf{p}\vec{m})^T \mathbf{w} (\vec{d} - \mathbf{p}\vec{m}) \quad \Rightarrow \quad \vec{m}' = \mathbf{c}\mathbf{p}^T\mathbf{w}\vec{d}, \;\; \mathbf{c} = (\mathbf{p}^T\mathbf{w}\mathbf{p})^{-1}$$

timestream

map

pointing matrix (map to timestream)

inverse of timestream noise covariance

max-L map estimator

map-space covariance matrix (constructed from timestream covariance matrix)

  - would need to include bolo-bolo correlations in timestream noise covar.
  - c requires inversion of $N_{pix}^2 = 16000^2$ matrix
- Simulation-based techniques have been used to deal with this
- We use hybrid method
  - Scan pattern ⇒ naive maps are pretty close to optimal for a single obs.
  - Stationarity of noise in each map ⇒ map covar. is diagonal in maps space, well describe by simple map PSD
  - Coadd observations in Fourier space with map PSD inverse var. weighting
  - Jackknifes and sims used to determine transfer function and uncertainties

Pseudo-Optimal Mapmaking

- Optimizing sky noise removal
  - Optimal sky noise removal algorithm depends on the day's weather
  - Pick algorithm (ave, planar, quadratic) based on single-obs figure of merit (essentially, single-obs variance on power spectrum bandpower)

$$\mathrm{FOM} = \sum_{\vec{\nu}} \frac{S_{\vec{\nu}}^2 W_{\vec{\nu}}^2 B_{\vec{\nu}}^2}{\mathcal{P}_{\vec{\nu}}^2} \qquad S_{\vec{\nu}} \propto \frac{1}{\ell(\ell+1)} \qquad W_{\vec{\nu}} B_{\vec{\nu}} = \text{transfer function}$$

(doesn't involve the real map, just the single-obs PSD)

  - Relative weights:

method	Fraction of obs	Fractional contribution to FOM
avg	50%	70%
planar	40%	29%
quadratic	10%	1%

  - Determine overall transfer function by weighted sum of single-obs transfer function

Coadd PSDs and Transfer Functions

- Final PSD determined from jackknife coadds: random signs on each observation
- Final coadd PSD
  - not white
  - But beautifully gaussian: deviations present in single obs gone

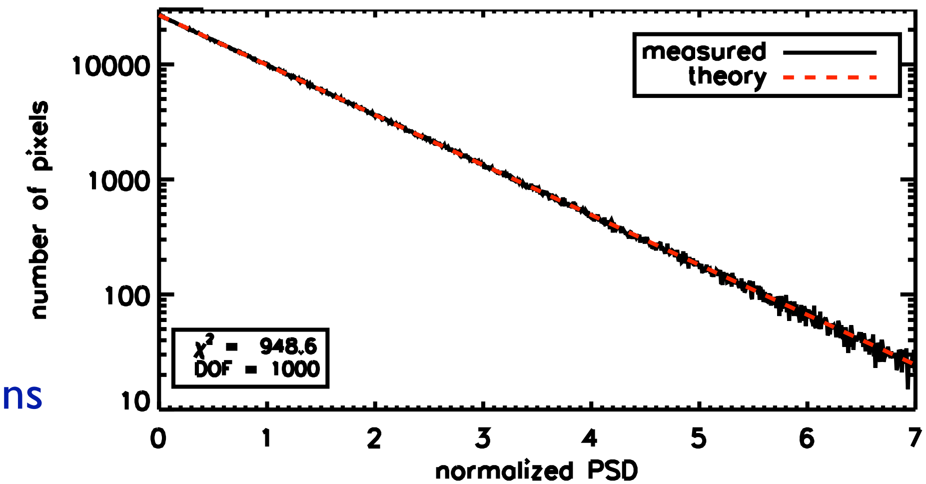

Coadd PSD

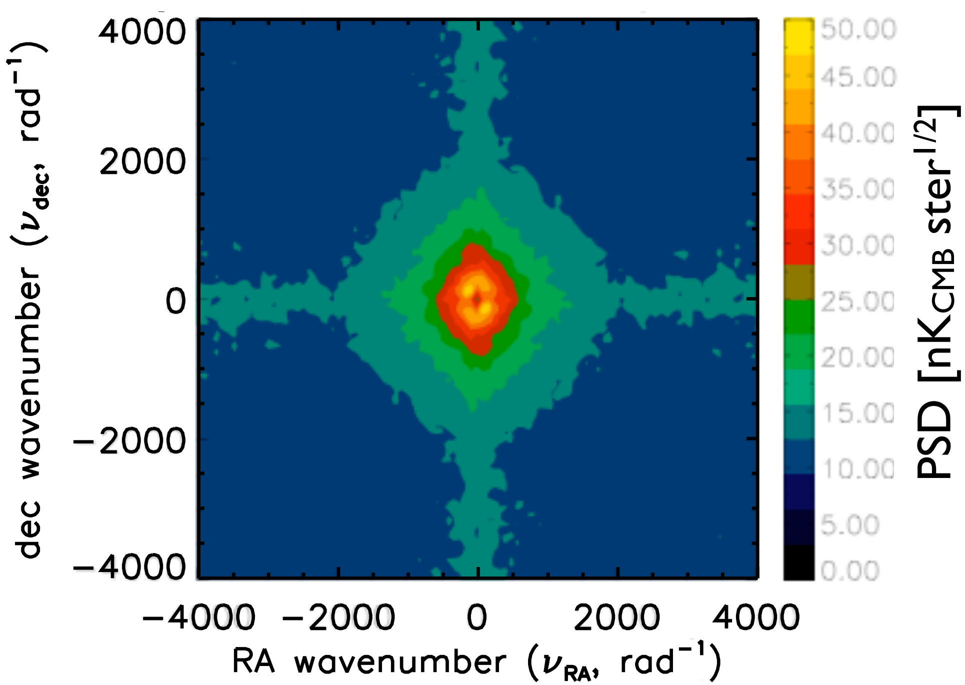

Coadd Transfer Function

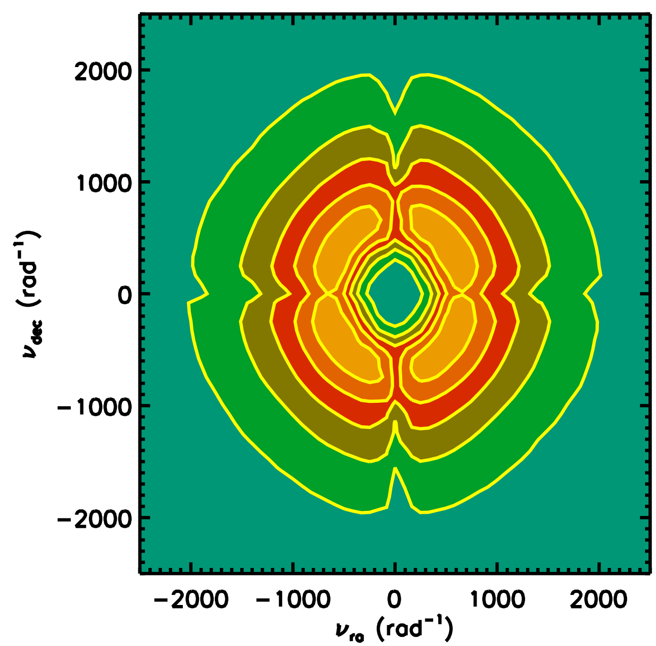

Coadd PSDs and Transfer Functions

- Final PSD determined from jackknife coadds: random signs on each observation
- Final coadd PSD
  - not white
  - But beautifully gaussian: deviations present in single obs gone

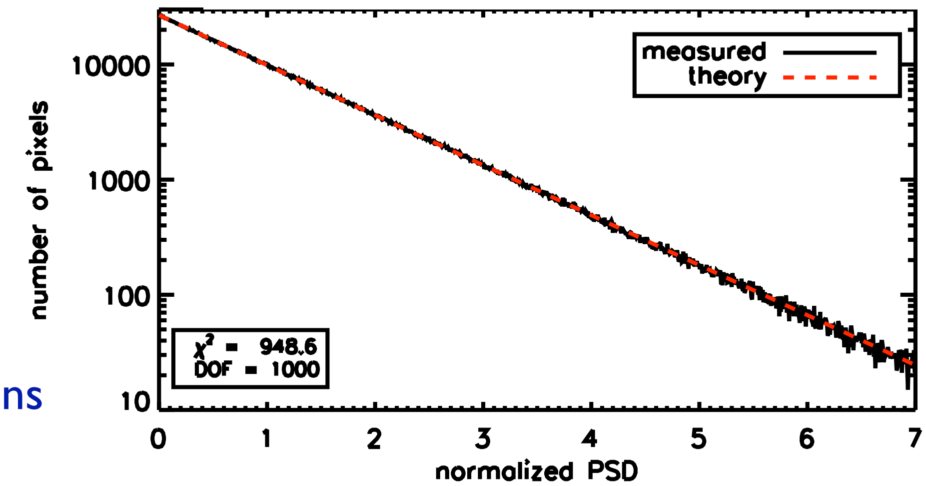

Coadd PSD

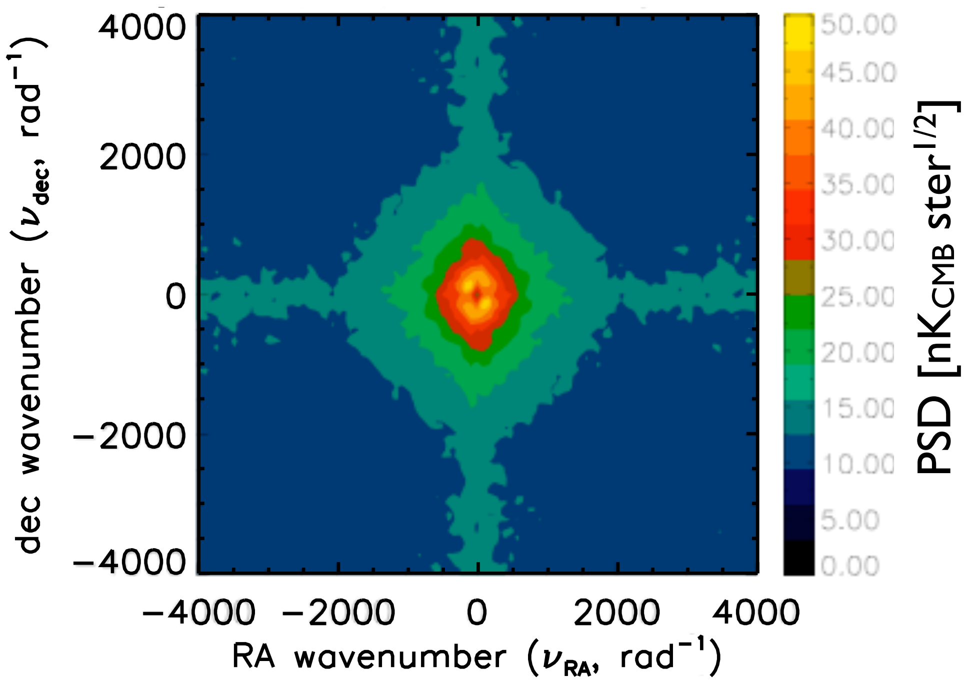

Coadd Transfer Function

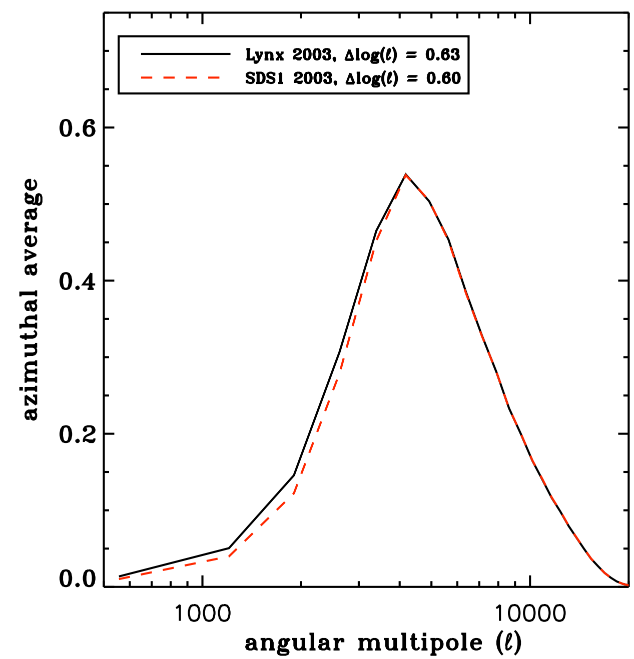

Total Anisotropy Power Spectrum Constraint

- Do we see excess noise power? Do Max L estimate of A, the amplitude of the flat bandpower anisotropy

$$\log(\mathcal{L}) = \sum_{\vec{\nu}} \left(-\log(\mathcal{P}_{\vec{\nu}} + AS_{\vec{\nu}}B_{\vec{\nu}}W_{\vec{\nu}}) - \frac{x_{\vec{\nu}}}{\mathcal{P}_{\vec{\nu}} + AS_{\vec{\nu}}B_{\vec{\nu}}W_{\vec{\nu}}} \right)$$

coadd PSD from jackknifes (noise estimate when no signal)

possible signal term

- Bayesian likelihood function width is v. approximate: correlations between Fourier modes puts in a covariance we have not included
- Use Feldman-Cousins to obtain correct frequentist confidence interval

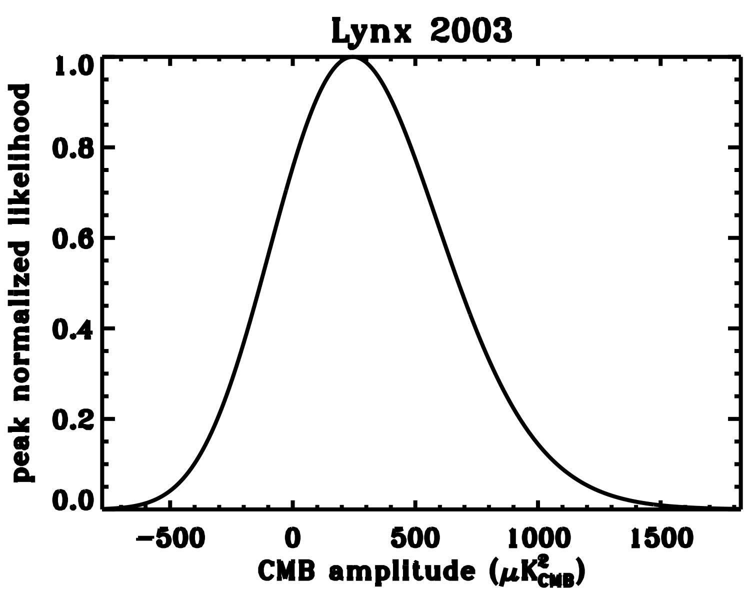

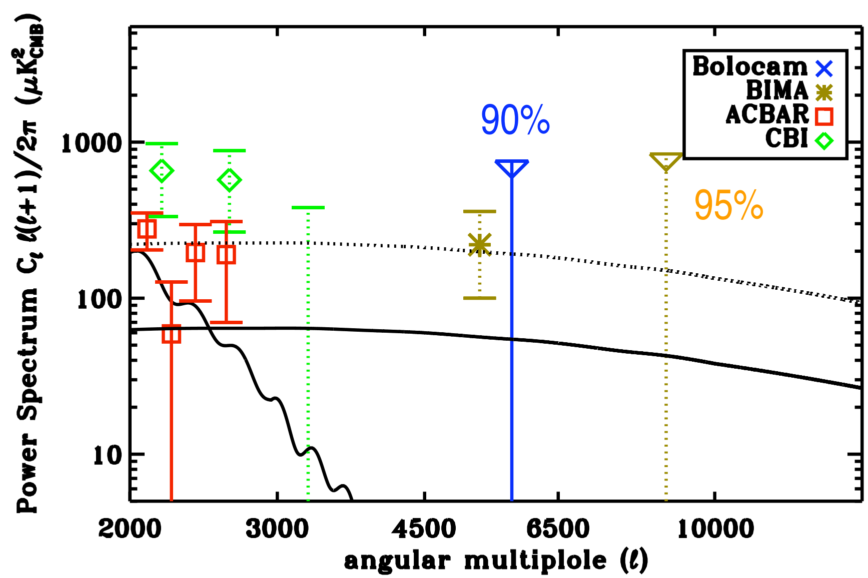

(Kuo *et al* 2007 ACBAR points)

SZ Anisotropy Power Spectrum Constraint

- No detection of anisotropy power
- Want to constrain amplitude of putative SZ anisotropy power spectrum
- Complications:
  - Need to include contribution of CMB, ~ 45 μK_{CMB}^2
    - Done properly by adding expected value to P_ν
    - CMB power spectrum from Spergel et al (2007) and Kuo et al (2007)
    - Fluctuations automatically accounted for by adding random CMB realization to each jackknife noise realization.
  - What is the SZ power spectrum? Use two models:
    - Flat bandpower like CMB
    - Komatsu and Seljak (2002) analytic spectrum
    - Other spectra in literature not very different in our ℓ range of interest

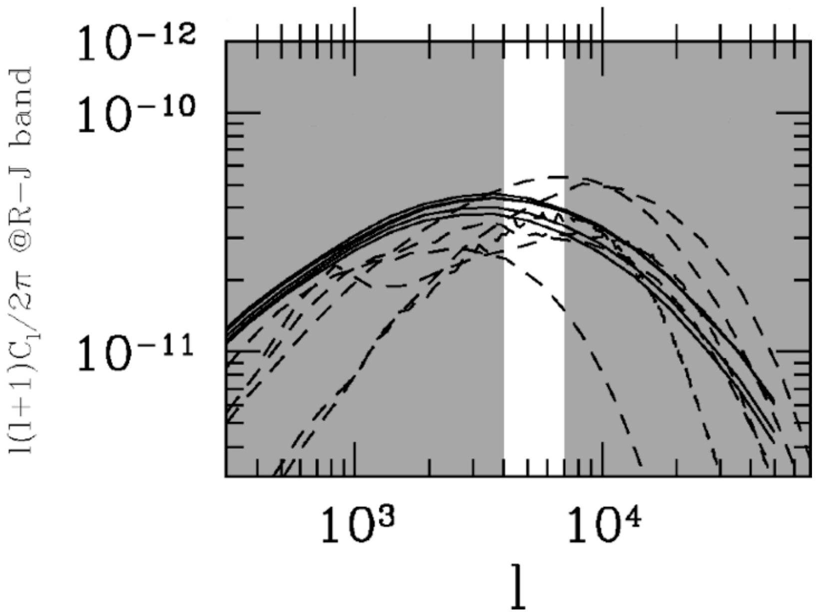

SZ Anisotropy Power Spectrum Constraint

- Constraints on amplitude of total and SZ anisotropy PS:

spectrum	flux uncertainty	68% CL interval	90% CL interval	95% CL interval	
flat-total	0	$99 - 588\ \mu K^2_{CMB}$	$0 - 755\ \mu K^2_{CMB}$	$0 - 828\ \mu K^2_{CMB}$	← total anisotropy
flat-SZE	0	$90 - 582\ \mu K^2_{CMB}$	$0 - 747\ \mu K^2_{CMB}$	$0 - 830\ \mu K^2_{CMB}$	SZ anisotropy
flat-SZE	3.5% (meas)	$89 - 634\ \mu K^2_{CMB}$	$0 - 794\ \mu K^2_{CMB}$	$0 - 876\ \mu K^2_{CMB}$	SZ anisotropy
flat-SZE	6.3% (total)	$83 - 692\ \mu K^2_{CMB}$	$0 - 956\ \mu K^2_{CMB}$	$0 - 998\ \mu K^2_{CMB}$	SZ anisotropy
KS-SZE	0	$77 - 543\ \mu K^2_{CMB}$	$0 - 686\ \mu K^2_{CMB}$	$0 - 766\ \mu K^2_{CMB}$	SZ anisotropy
KS-SZE	3.5% (meas)	$76 - 569\ \mu K^2_{CMB}$	$0 - 741\ \mu K^2_{CMB}$	$0 - 834\ \mu K^2_{CMB}$	SZ anisotropy
KS-SZE	6.3% (total)	$73 - 732\ \mu K^2_{CMB}$	$0 - 950\ \mu K^2_{CMB}$	$0 - 993\ \mu K^2_{CMB}$	SZ anisotropy

  - 3 rows: no flux uncertainty, internal flux cal uncertainty, and full flux uncertainty (incl. uncertainty on external Mars model)
- SZ anisotropy scales as $\sigma_8^7(\Omega_b h)^2$
- Expected SZ anisotropy PS, using Dunkley et al (2008) cosmo params: 10 μK_{CMB}^2
- Using K-S spectrum and $\Omega_b h$ from Dunkley et al (2008) and Kuo et al (2007), we set limit of $\sigma_8 < 1.55$ at 90% CL
  - σ_8 = 0.80-0.85 from primary PS + LSS, σ_8 = 0.95 from high-ℓ

What Happened?

- Why did the survey end up being so unconstraining?
  Sky noise, sky noise, sky noise
  - In hindsight, old SuZIE data is suggestive that spatial correlations are not simple enough to be fully removable
  - But no real measurements of atmospheric correlation function, not even from SCUBA
  - We have studied sky noise on Mauna Kea more exhaustively than anyone before (Sayers et al 2008, in prep)

Thoughts on SZ Surveys

- On sky noise:
  - The sites for APEX, ACT, and SPT are better: Atacama and South Pole
  - But: even ACBAR saw sky noise at South Pole.
  - Possible sensitivity degradations
    - APEX and SPT: 2(f/#)λ horns, so no Airy function coupling. Other degradations though:
      - imperfect correlation of atmosphere, leaving 1/f noise in timestreams
      - transfer function of sky noise removal will hurt sensitivity
    - ACT: 0.5(f/#)λ bare absorber pixels; depending on how good or bad the atmosphere, may end up in same boat, with many fewer effective pixels, + above degradations

What Next?

- Bolocam
  - observing single massive clusters in raster mode has never been feasible because fields are too small: spend all the time turning around
  - we have learned how to observe single massive clusters in an efficient Lissajous scan mode, developed for SHARCII 350 μm CSO camera
  - would like to compare to OVRO/BIMA and SZA maps, resolve the discrepancies with SuZIE data

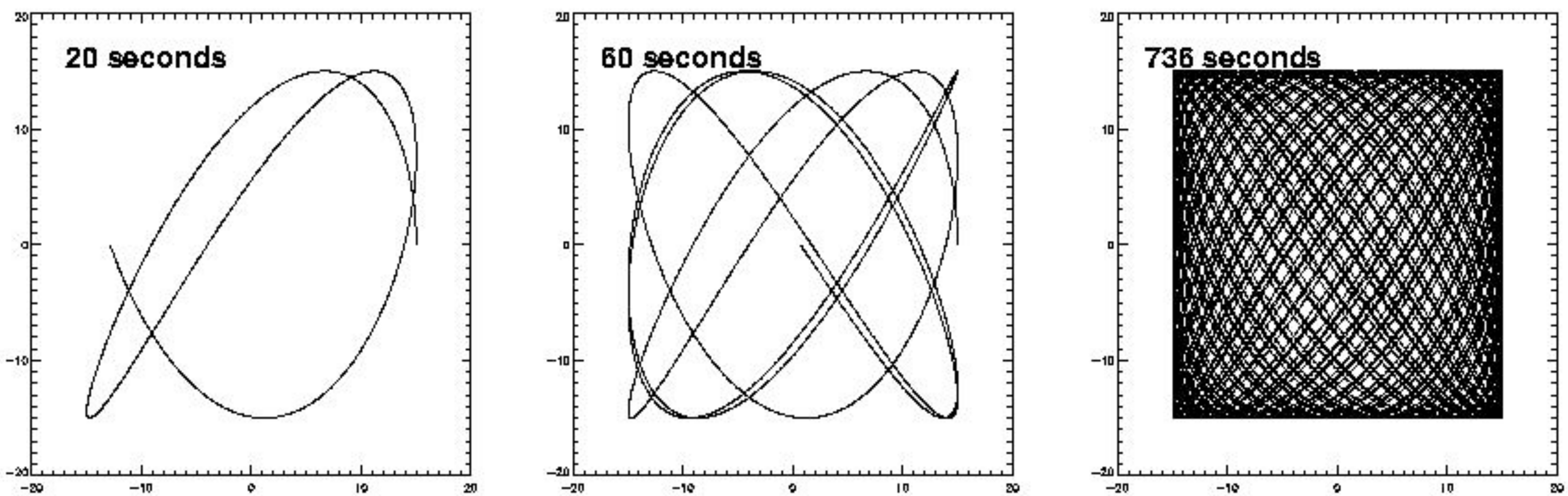

What Next?

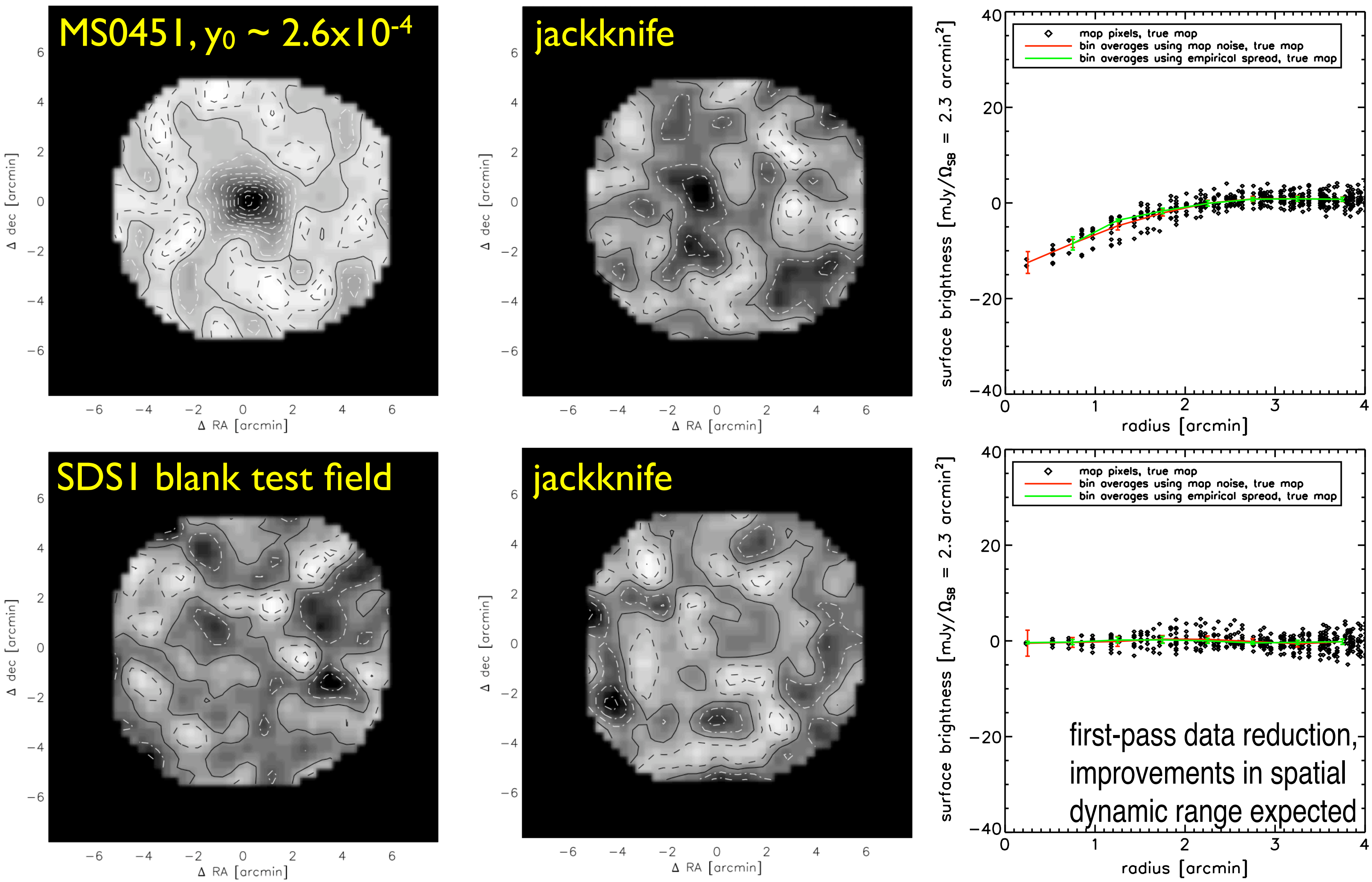
MS0451, $y_0 \sim 2.6\times10^{-4}$
jackknife
SDS1 blank test field
jackknife
Δ RA [arcmin]
Δ dec [arcmin]
map pixels, true map
bin averages using map noise, true map
bin averages using empirical spread, true map
surface brightness [mJy/Ω_{SB} = 2.3 arcmin^2]
radius [arcmin]
first-pass data reduction, improvements in spatial dynamic range expected

What Next?

- MKID camera for CSO
  - New technologies enable 4-color camera with 8' FOV (750 μm - 1.3 mm, possibly extend to 2 mm)
  - *Spectral sky subtraction*: each spatial pixel observes in multiple colors, so atmosphere can be regressed out
    - SuZIE II showed that this works beautifully for 4 spatial pixels
    - But large simultaneous 4-color focal plane not feasible 7 years ago
    - No worries about spatial correlations, though need to be sure source is orthogonal to atmosphere (it is for SZ)
  - Massive SZ cluster observations in Lissajous mode
- LWCam for CCAT
  - New 25-m submm/mm telescope in Chile
  - 5 or 6-color 750 μm - 2 mm camera in planning
  - High-resolution multicolor followup of clusters discovered in large area SZ surveys, again using Lissajous mode
  - Reach SZ-confusion limit

Submm/mm MKID Camera

- Antenna coupled MKIDs, in-line bandpass filters to obtain four colors/ spatial pixel (220, 275, 350, 420 GHz)
- 8' FOV, 600 spatial pixel, on CSO 2010
- 16-pixel/2-color DemoCam fielded